

Reservoir Facies Architecture in a Microtidal Barrier System— Frio Formation, Texas Gulf Coast

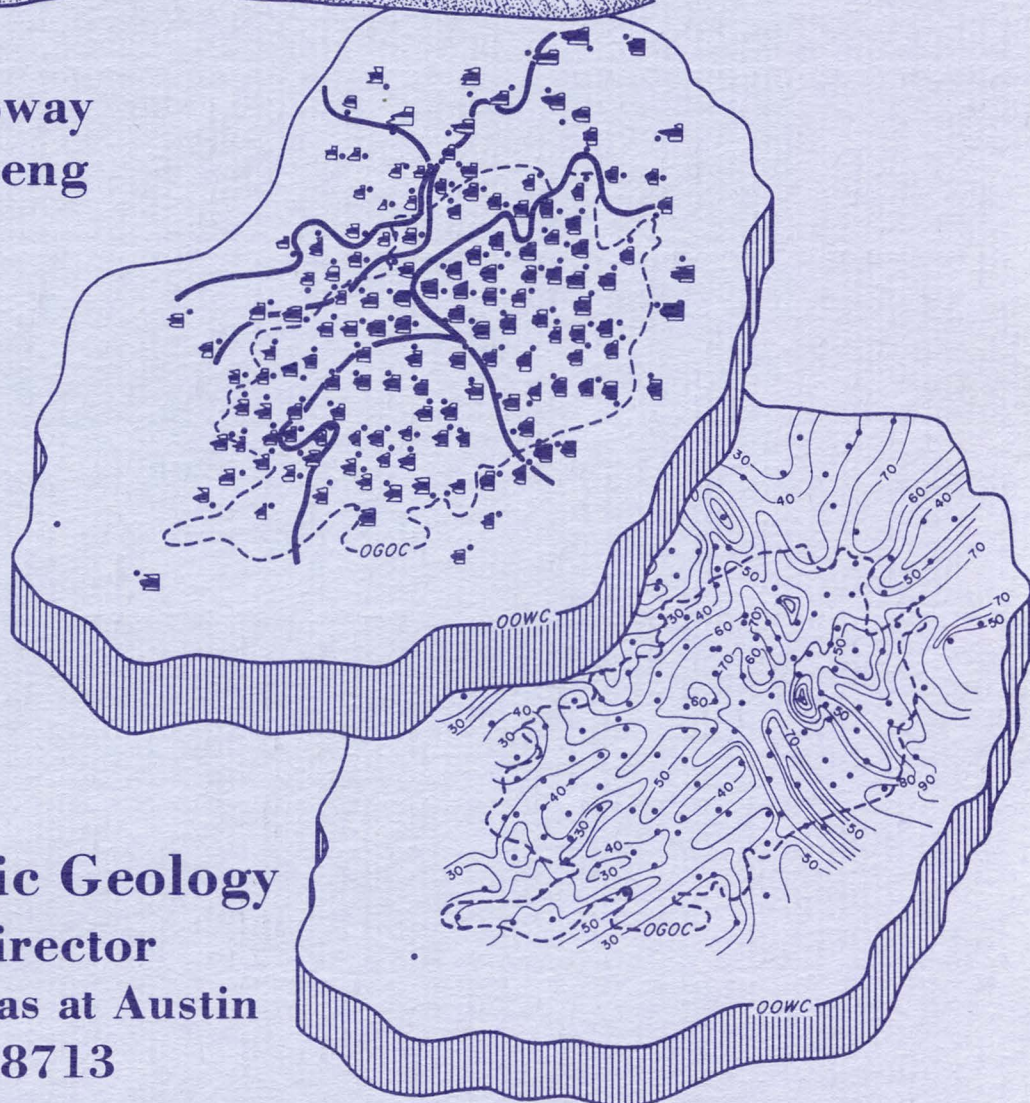
William E. Galloway
Eric Siu-Sien Cheng



1985



Bureau of Economic Geology
W. L. Fisher, Director
The University of Texas at Austin
Austin, Texas 78713



Report of Investigations No. 144

Reservoir Facies Architecture in a Microtidal Barrier System— Frio Formation, Texas Gulf Coast

**William E. Galloway
Eric Siu-Sien Cheng**



1985



**Bureau of Economic Geology
W. L. Fisher, Director
The University of Texas at Austin
Austin, Texas 78713**

CONTENTS

ABSTRACT	1
INTRODUCTION	1
Barrier-island depositional systems	3
Stratigraphic record of barrier deposition	4
Recognition of subsurface barrier facies	5
OIL-PRODUCTIVE SHORE-ZONE SYSTEMS OF THE GULF BASIN	6
West Ranch field	7
41-A reservoir—a progradational barrier sandstone	10
Component barrier-island facies	14
Barrier-core facies	14
Inlet-fill facies	14
Lateral facies relationships	16
Overview of reservoir facies heterogeneity	17
Permeability distribution	17
Resistivity patterns and hydrocarbon distribution	19
Drainage history	22
Greta reservoir—an aggradational barrier sandstone	23
Reservoir characteristics and origin	23
Production history	26
Glasscock reservoir—a transgressive barrier sandstone	27
Reservoir characteristics and origin	27
Hydrocarbon distribution and production history	29
DISCUSSION AND CONCLUSIONS	30
ACKNOWLEDGMENTS	35
REFERENCES	35
APPENDIX	36

FIGURES

1. Microtidal, wave-dominated shore-zone depositional systems	2
2. Depositional environments of a microtidal barrier island, Matagorda Island, Texas coast	3
3. Architectural elements of a barrier-island sand body	4
4. Stratigraphy of progradational, aggradational, and transgressive barrier-island sand bodies	5
5. Sand-body geometry and representative SP logs of modern barrier islands of the Texas coast	6
6. Depositional systems of the Frio Formation and paleogeographic setting of West Ranch field	7
7. Structure-contour map of West Ranch field showing the simple domal anticline that creates the trap	8
8. Dip-oriented regional cross section through West Ranch field	9
9. Structure-contour map of West Ranch field showing the combined domal structure and superimposed depositional topography of the 41-A reservoir	11

10. Net-sand isolith map of the 41-A main and the genetically associated stringer reservoir	12
11. Map of SP log patterns of the 41-A sand	13
12. Interpreted depositional elements of the 41-A sand	15
13. Log response, texture, internal features, and petrophysical properties of the barrier-core facies of the 41-A reservoir, well A-493	15
14. Log response, texture, internal features, and petrophysical properties of the inlet-fill facies, 41-A reservoir, well A-496	16
15. Map of average 41-A reservoir permeability	18
16. Cross plot of measured core-plug permeability (k) and log-derived deep resistivity (R_t) within the hydrocarbon-saturated zone of the 41-A reservoir	19
17. Deep-resistivity log patterns of the hydrocarbon-saturated portion of the 41-A reservoir	20
18. Geometries of resistivity (saturation) compartments	21
19. Water-cut distribution in test wells during latter stages of depletion of the 41-A main reservoir	22
20. Typical log response and textural properties of the Greta reservoir, well A-493	24
21. Map of deep-resistivity log patterns in hydrocarbon saturated portions of the Greta reservoir	25
22. Distribution of maximum measured deep resistivity within hydrocarbon-saturated portions of the Greta reservoir	25
23. Map of water-cut for wells producing in the Greta reservoir, June 1977	26
24. Log response, internal features, and petrophysical properties typical of the Glasscock reservoir	27
25. Net-sand isolith map of the Glasscock reservoir	28
26. Interpreted depositional elements of the Glasscock sand in the main field area	29
27. Geometry of water-flood front following 9 years of water injection along the gas-oil contact	30
28. Reservoir model of the barrier-core and inlet-fill facies complex	32
29. Reservoir model of tidal-channel fill and associated tidal-delta and back-barrier facies mosaic	33
30. Reservoir model of washover-fan and associated back-barrier facies	34

TABLE

1. Characteristics of the Greta, Glasscock, and 41-A reservoirs, West Ranch field	10
---	----

PLATES (in pocket)

1. Cross sections through 41-A reservoir, West Ranch field area
2. Resistivity (saturation) compartments and reservoir architecture

ABSTRACT

Sandstone reservoirs deposited in microtidal barrier systems contain large oil and gas reserves in several Gulf Coast Basin plays. Three representative Frio Sandstone reservoirs in West Ranch field show that barrier-island sand bodies are complex mosaics of barrier-core, inlet-fill, flood-tidal-delta, washover-fan, barrier-flat, and shoreface facies. The proportions of these facies differ within progradational, aggradational, and transgressive barrier sand bodies. Detailed isolith and log-facies maps, based on closely spaced production wells, combined with analysis of resistivity distribution and sparse core control, provide the basis for interpretation of the 41-A, Glasscock, and Greta reservoirs.

The 41-A reservoir is a progradational barrier sand body. The most important producing facies include the barrier core and crosscutting inlet fill. Permeability and distribution of irreducible water saturation reveal depositional patterns and subdivisions of the sand body into numerous facies-controlled compartments. Both original hydrocarbon saturation and irregularities in water encroachment show that the facies compartments locally affect fluid movement within the reservoir.

The Greta reservoir is an aggradational barrier complex. This massive sand body consists of intermixed barrier-core and inlet-fill units. Prominent resistivity compartments are dip oriented, indicating the importance of inlet development during barrier aggradation. Despite the uniform appearance of the Greta reservoir, water encroachment has been irregular.

The Glasscock reservoir is characterized by comparatively low permeability and is an atypically thin and discontinuous Frio reservoir. It is interpreted to be a transgressive barrier deposit, and it consists mainly of large washover-fan and associated barrier-flat sands. Hydrocarbon saturation, drainage, and injection response all reflect the facies geometry typical of a transgressive barrier complex.

Recovery efficiency of Frio barrier-island reservoirs is high. However, projected primary and secondary recovery from the three reservoirs studied range from 56 percent of oil in place in the 41-A reservoir to 39 percent in the Glasscock sandstone. The Greta sandstone is intermediate, having a projected recovery of 42 percent of oil in place.

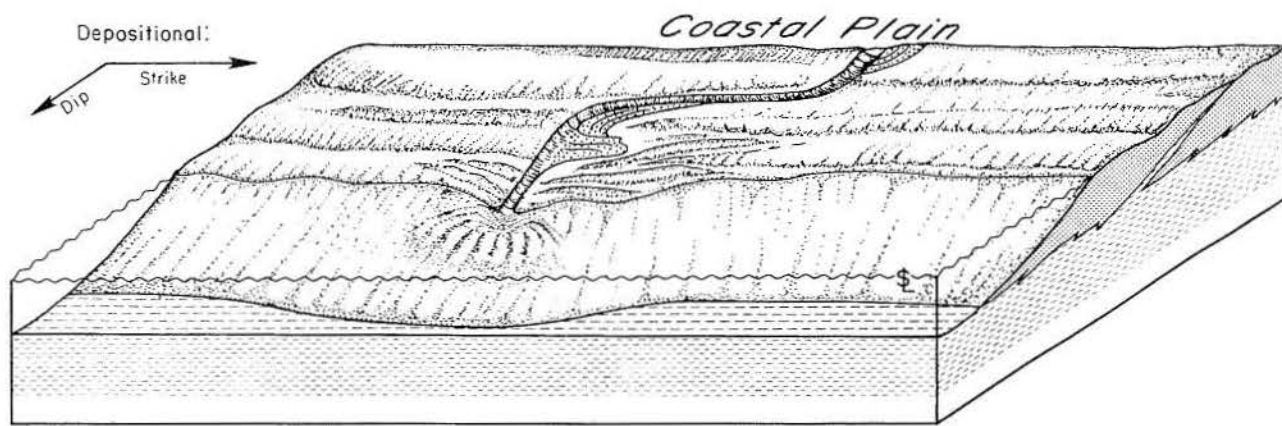
Keywords: barrier bar, barrier inlet, enhanced recovery, Frio Formation, petroleum, natural gas, reservoirs

INTRODUCTION

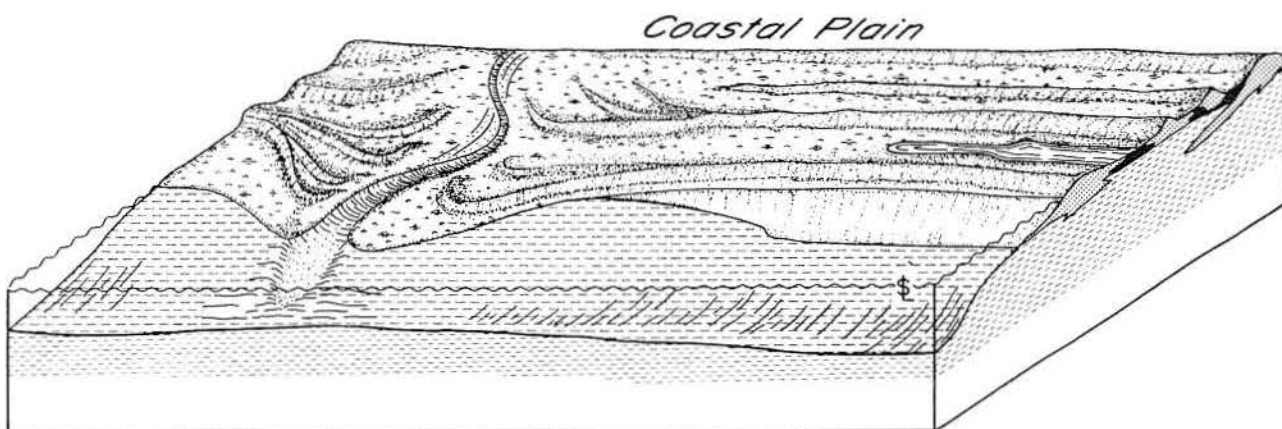
Sand bodies of interdeltaic shore-zone depositional systems are important hydrocarbon reservoirs in the northwestern Gulf Coast and many other basins. In intracratonic basins and smaller oceanic basins, such as the Gulf of Mexico, tidal range is commonly limited, and shore-zone sedimentation is dominated by wave processes. Along such microtidal wave-dominated shorelines, the depositional variability of framework sand bodies is determined by coastal physiography, sediment texture, and rates of sediment supply relative to base-level change. Three major varieties of wave-dominated, microtidal, shore-zone depositional systems can be differentiated (Morton and McGowen, 1980; Galloway and

Hobday, 1983): sand-rich strandplains, mud-rich strandplains (cheniers), and barrier islands. In strandplains, the shore zone and associated shoreface are attached to the subaerial coastal plain (fig. 1A, 1B).

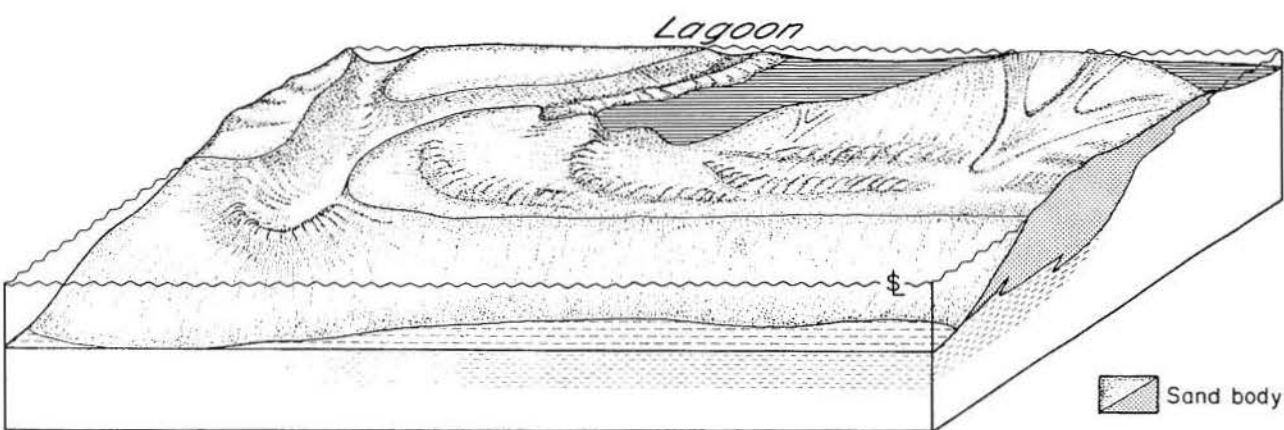
This report discusses the petroleum reservoir geology of one typical barrier-island/lagoon depositional system (fig. 1C) in order to (1) document the effects of barrier sand-body complexity on oil recovery and (2) illustrate approaches that may be applied to improve geologic description and exploitation of barrier reservoirs. Facies variability and reservoir attributes of strandplain systems are described in a companion report by Tyler and Ambrose (in press).



A. Sand-Rich Strandplain



B. Mud-Rich Strandplain (Chenier Plain)



C. Barrier Island

QA-2274

Figure 1. Microtidal, wave-dominated shore-zone depositional systems. A. Sand-rich strandplain. B. Mud-rich strandplain (chenier plain). C. Barrier island.

Barrier-Island Depositional Systems

Barrier islands lie offshore of and are separated from the adjacent coastal plain by a series of lagoons or bays (fig. 1C). Presence of the protected water body behind the barrier and resultant exchange of lagoonal and oceanic water, with even the modest rise and fall of the tide on microtidal coasts, create a complex of environments within the barrier system. These environments and the resultant genetic facies reflect the physiography of a barrier island (fig. 2) (Morton and McGowen, 1980; Heron and others, 1984). They include (1) the barrier core, or axis; (2) crosscutting inlets and their infill sediments; (3) back-barrier flood-tidal deltas, storm-generated washover fans, and barrier flats; and (4) fore-barrier shoreface and ebb-tidal deltas. The individual barrier-bar sand body may thus be viewed as a three-dimensional jigsaw puzzle (fig. 3).

The *barrier core* is the strike-elongate, massive sand skeleton of the barrier. The core is a composite of well-sorted beach, dune, and upper-shoreface sands. Internal bedding or obvious depositional architecture is poorly developed, but low-angle seaward imbrication of successive barrier-core units may be distinguished (fig. 3).

Inlet fill consists of stubby, dip-oriented, erosionally bounded deposits that accumulated along the updrift margin by the combined processes of inlet incision, longshore migration of the inlet throat, and filling by spit accretion. Internal depositional architecture reflects the

longshore accretion of the tip of the updrift barrier island (fig. 2). The fill facies is characterized by (1) an erosional base and basal lag consisting of shell or other coarse debris; (2) an upward-fining textural sequence, which reflects the channel infilling; (3) a superimposed upward-coarsening sequence, reflecting the lateral accretion of the spit platform; and (4) a cap of beach deposits along the updrift inlet margin.

Flood-tidal-delta sands lie on the lagoonal side of the inlet fill. The facies consists both of thin, upward-coarsening progradational sequences produced by sediment washed through the inlet into the shallow water of the lagoon and of crosscutting, lenticular tidal-channel fills. The overall sedimentary unit is lobate and pinches out landward into fine-grained lagoonal fill.

Washover-fan and barrier-flat deposits form a landward-thinning apron along the lagoonal side of the barrier core (fig. 2). Thin, upward-coarsening, progradational units are capped by variable thicknesses of horizontally bedded, aggradational washover, eolian, tidal-flat, and marsh sands. Thin washover channel fills crosscut the aggradational sequence.

The *shoreface* forms the seaward margin of the barrier core. In microtidal barriers, the ebb-tidal delta is poorly developed and is rarely differentiated from the shoreface. Shoreface deposits are characterized by low-angle, seaward-dipping bedding, an upward-coarsening textural sequence, and gradational contacts basinward and downward into open-marine shelf muds. As in the barrier core, depositional grain is strike parallel.

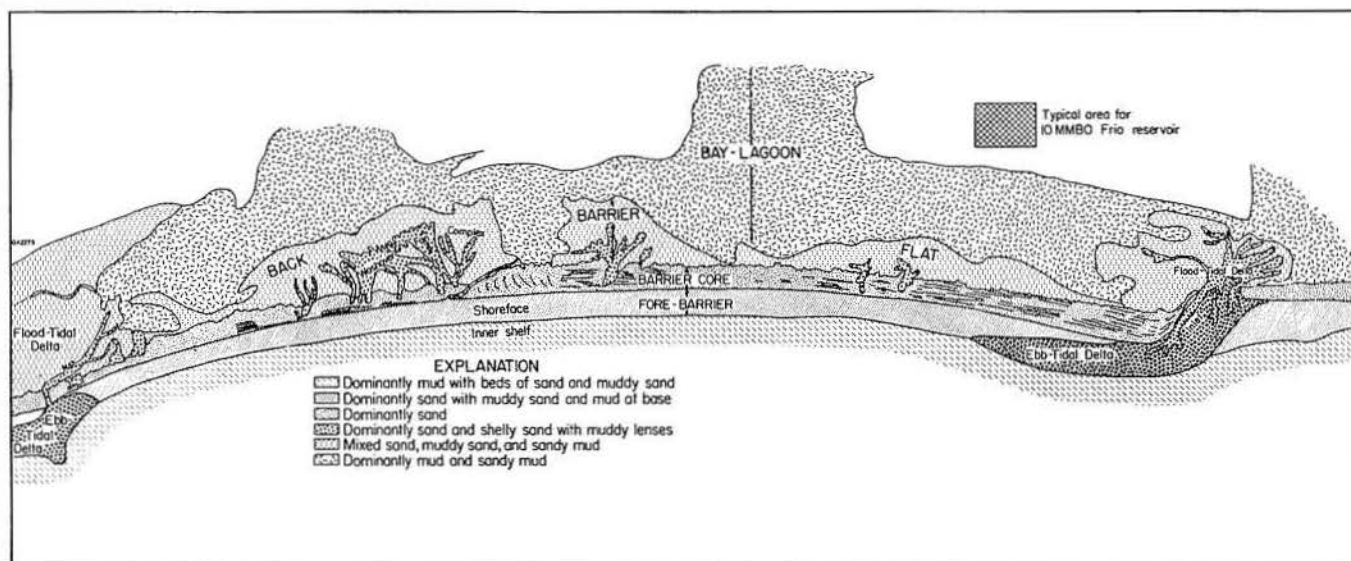


Figure 2. Depositional environments of a microtidal barrier island, Matagorda Island, Texas coast.

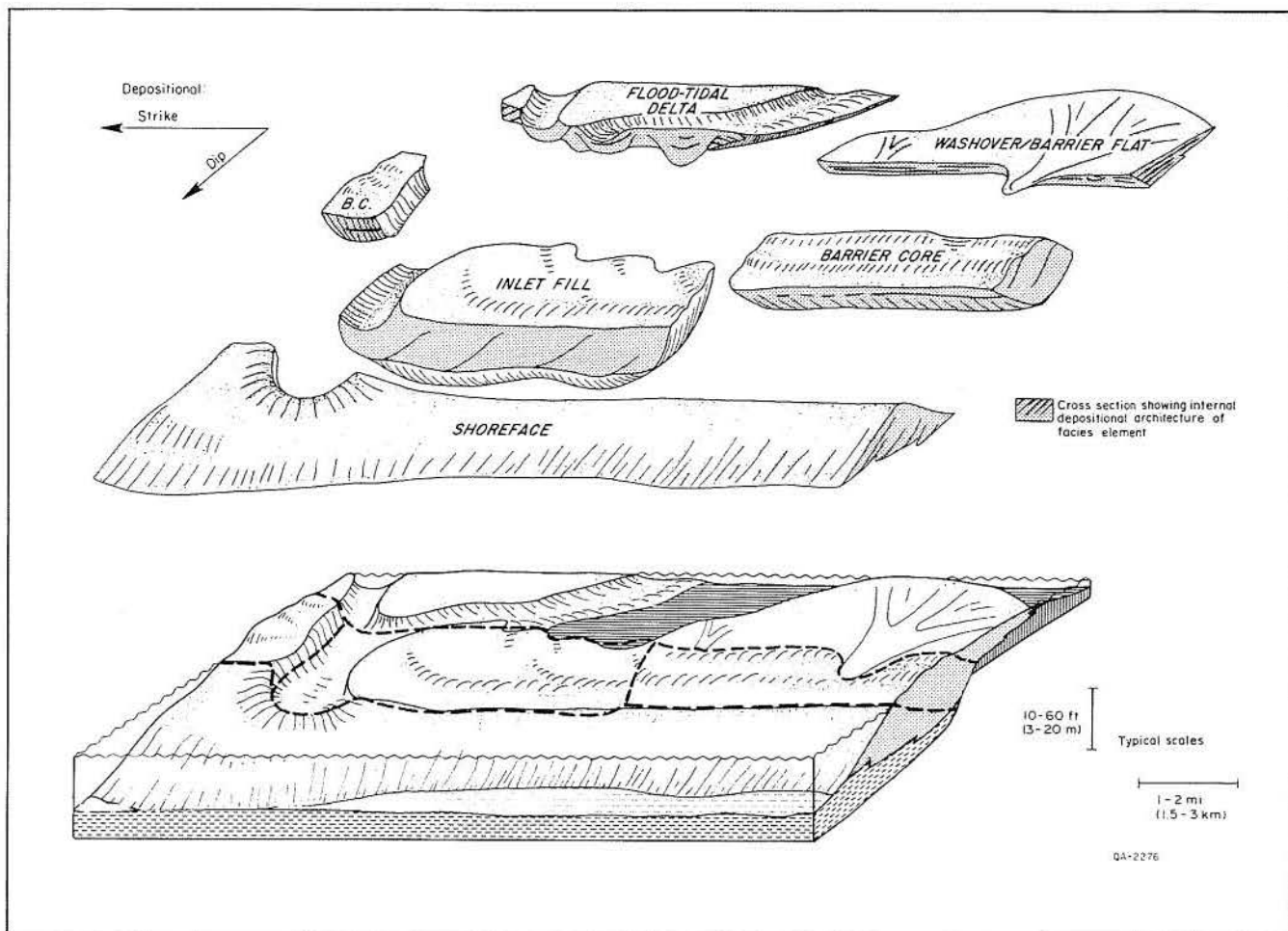


Figure 3. Architectural elements of a barrier-island sand body.

Stratigraphic Record of Barrier Deposition

The proportion and lateral distribution of the component facies of barrier islands are determined by the relative rates of sediment supply and of base-level change (Wilkinson, 1975; Morton and McGowen, 1980). Where sediment input exceeds submergence (whether because of subsidence or eustatic sea-level rise), barriers prograde, forming laterally extensive sand belts containing well-preserved shoreface facies sequences with superposed barrier-core and back-barrier deposits (fig. 4A). In prograded barrier-island sand bodies, lateral separation of barrier-core facies and crosscutting inlet-fill facies is pronounced.

Where the position of a barrier complex is stabilized by a balance between sediment input and relative base-level rise, thick, vertically amalgamated, aggradational barrier sand bodies may form (fig. 4B). Barrier-core and inlet-fill

sands dominate the facies mosaic; inlet-fill deposits attain increased volumetric importance at the expense of shoreface and back-barrier facies.

Where relative rise in base level exceeds sediment supply, barrier aggradation can no longer keep pace, and the barrier shoreline shifts landward. In such a transgressive setting, the barrier retrogrades landward by storm washover and tidal flooding into the shallow, protected water of the lagoon (Kraft and John, 1979; Penland and Suter, 1983; Heron and others, 1984). The shoreface is a zone of erosion. As a result, back-barrier facies and multiple, localized inlet fills constitute the bulk of the preserved sand body (fig. 4C). Resulting sequences are typically thin and volumetrically small; they may be capped by upward-fining textural trends that reflect transgression and increasingly deep water environments. Sand bodies are isolated within lagoonal and marine muds.

MICROTIDAL BARRIER-ISLAND DEPOSITIONAL ARCHITECTURE

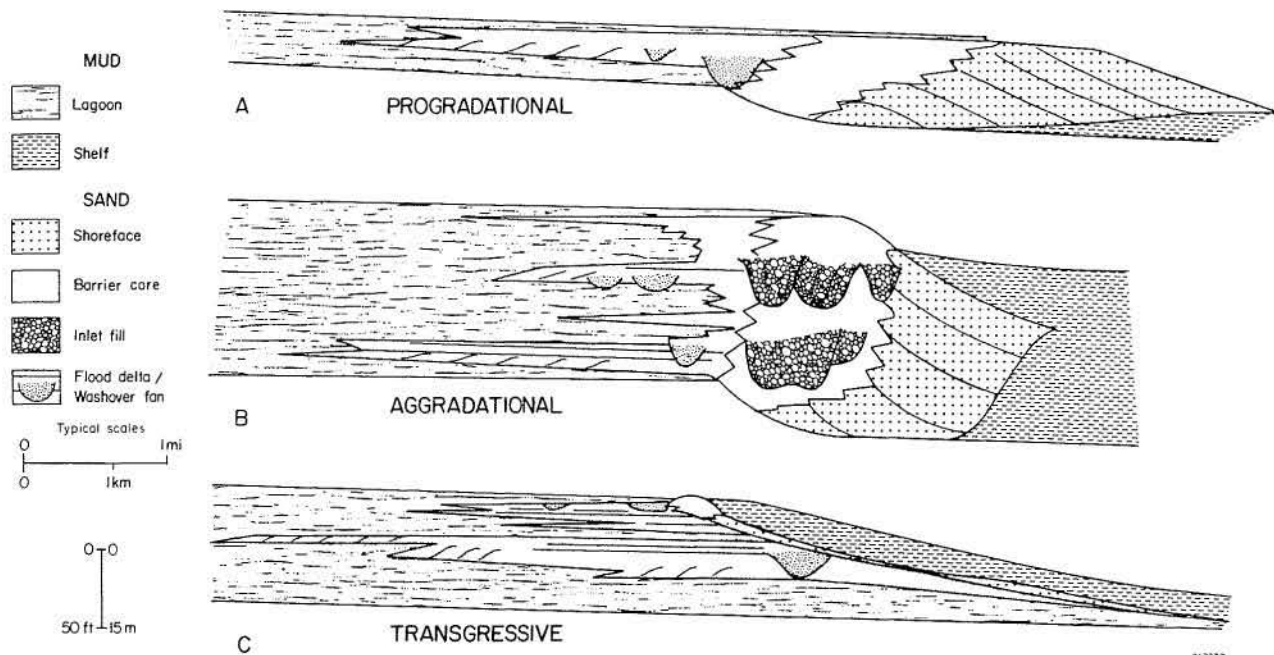


Figure 4. Stratigraphy of (A) progradational, (B) aggradational, and (C) transgressive barrier-island sand bodies.

Recognition of Subsurface Barrier Facies

Barrier-island facies are distinguished by composite sand-body geometry, vertical textural sequences, nature of boundaries with underlying or surrounding facies, bedding architecture, and internal sedimentary structures. Sand-body geometries of modern microtidal barrier islands of the Texas coast were illustrated by Bernard and others (1970) and Wilkinson (1975). Geometry and typical sand-body thicknesses are shown by isolith maps of Galveston and Matagorda Islands (fig. 5). Both islands are moderately progradational barriers. The simple, strike-parallel contours of the barrier core and associated shoreface are complicated by both inlet-fill and back-barrier facies. Geophysical log patterns,

illustrated by Bernard and others (1970) and shown in figure 5, are particularly useful indicators of contrasting textural sequence, bedding, and vertical facies relations. Shoreface, inlet-fill, and back-barrier-flat sequences have characteristic profiles.

Where core is available, primary and biogenic sedimentary structures guide interpretation of specific barrier facies. Reviews include papers by Kumar and Sanders (1974), Hayes and Kana (1976), Hubbard and others (1979), Kraft and John (1979), Morton and McGowen (1980), and Galloway and Hobday (1983).

As will be shown in this report, detailed examination of sand-body geometry, log-pattern distribution, and limited core information can define internal facies composition of barrier-bar reservoirs.

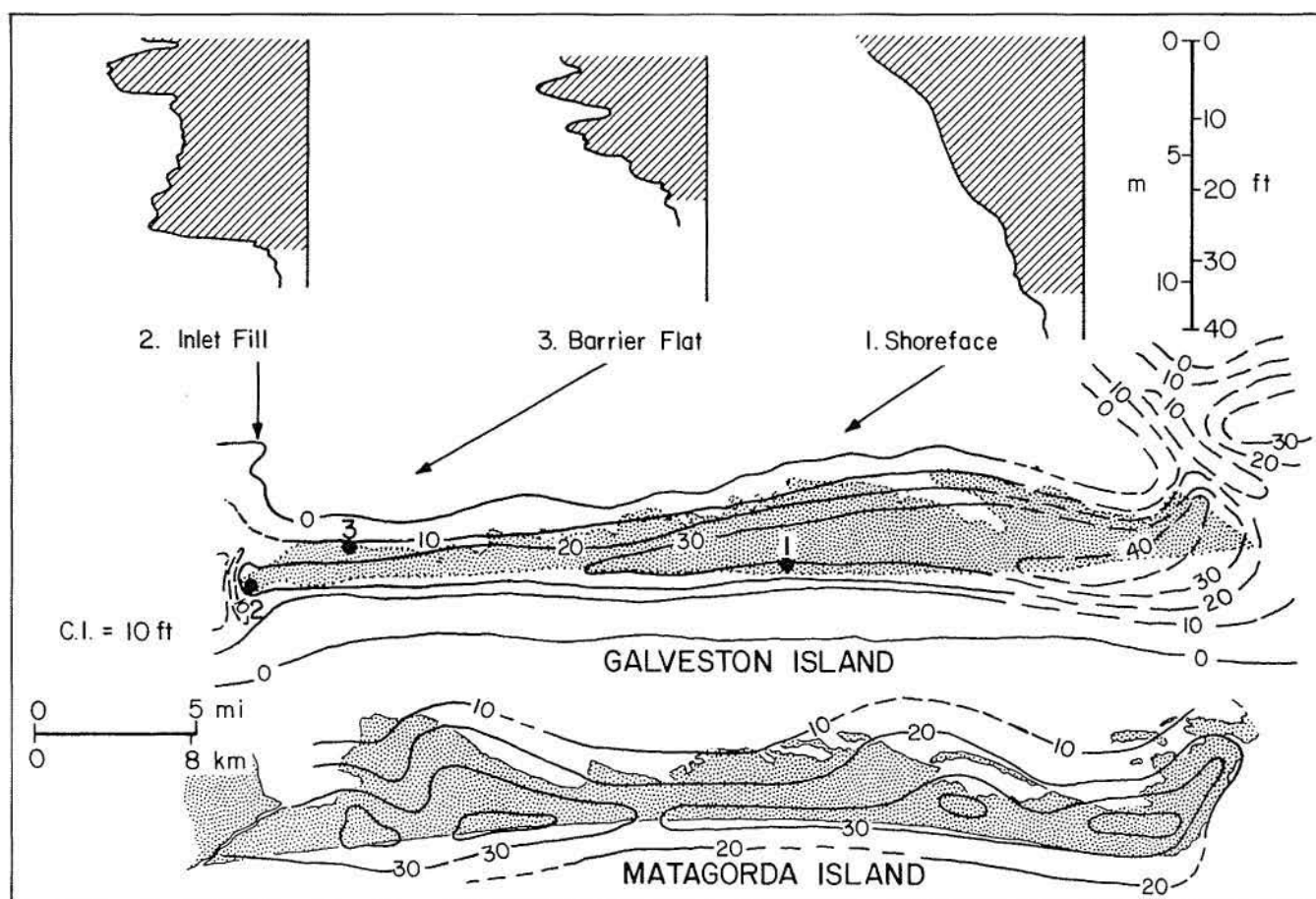


Figure 5. Sand-body geometry and representative SP logs of modern barrier islands of the Texas coast. Note effect of major inlets on isolith patterns. Compiled from Bernard and others (1970) and Wilkinson (1975).

OIL-PRODUCTIVE SHORE-ZONE SYSTEMS OF THE GULF BASIN

Three major oil-productive plays of the Texas Coastal Plain occur in barrier/strandplain depositional systems (Galloway and others, 1983). The Buna and Greta/Carancahua systems of the Frio Formation (Oligocene) and the Jackson-Yegua (Eocene) system contain productive barrier-island and strandplain sand bodies. The Greta/Carancahua (fig. 6) contains the largest play and has proved to be a prolific producer of both gas and oil. Estimated oil in place in reservoirs that have individually produced more than 10 million barrels exceeds 4.2 billion barrels (Galloway and others, 1983). Production has included nearly 3 billion barrels of liquids and 23 Tcf of gas (Galloway and others, 1982). More than 80 percent of the oil is pooled along the updip, landward margin of the barrier/strandplain trend (play VI in Galloway and others [1982]).

Oil recovery efficiency is high in the Frio barrier/strandplain reservoirs. A strong natural water drive and high porosity (averaging more than 30 percent) and permeability (commonly exceeding 1 D) combine to allow recovery of more than 50 percent of the oil in place in many reservoirs.

The Eocene Jackson-Yegua barrier/lagoon depositional system of the South Texas Coastal Plain contains nearly 1.2 billion barrels of oil in place in reservoirs that have produced more than 10 million barrels. However, lower average oil gravity and less efficient solution-gas drive combine to limit average recovery to 38 percent of the oil in place (Galloway and others, 1983).

Thus shore-zone sands constitute a prolific oil-producing setting, particularly if the reserves of numerous beach and barrier sandstone reservoirs

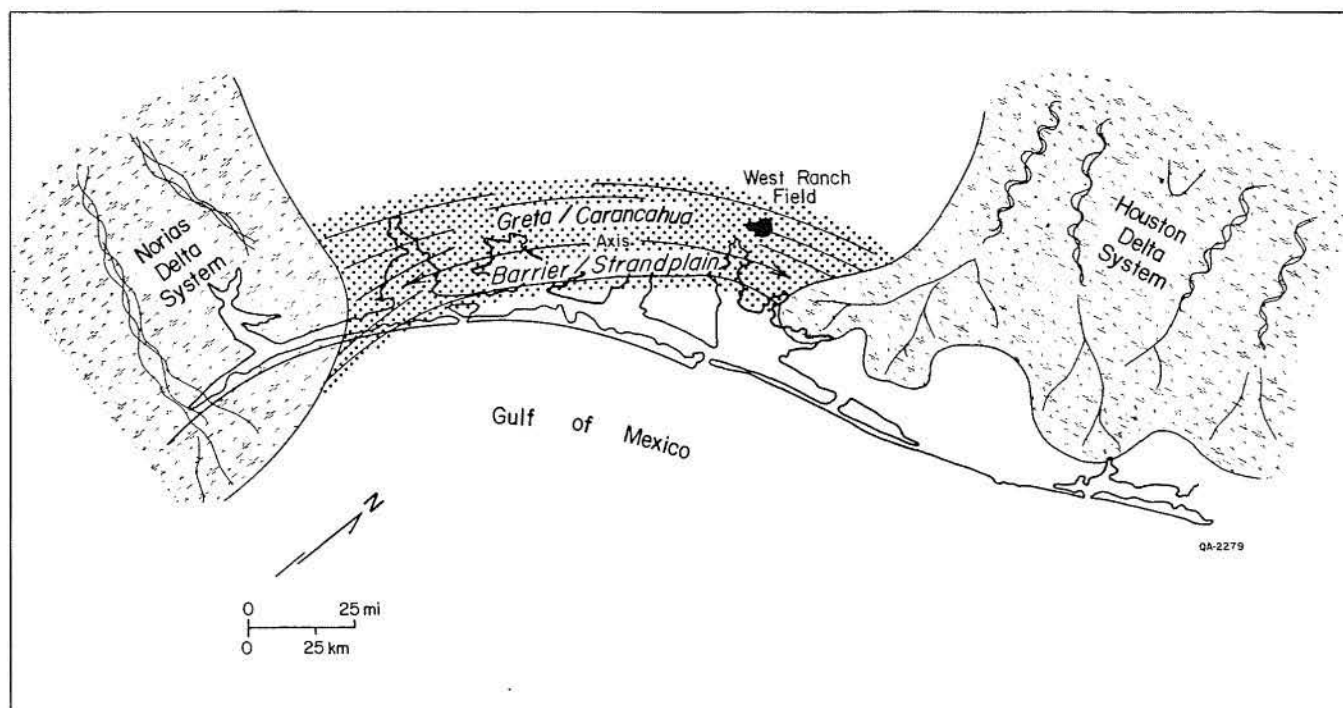


Figure 6. Depositional systems of the Frio Formation and paleogeographic setting of West Ranch field.

contained within the many Tertiary and Mesozoic deltaic systems are added to the 5 billion barrels of in-place oil found in these two large plays. West Ranch field, a major multipay oil and gas field of the Frio barrier/strandplain system, provides a natural laboratory for dissection of barrier-island reservoirs and their component facies.

West Ranch Field

West Ranch field lies along the northeastern end of the Frio Greta/Carancahua barrier/strandplain system (fig. 6). As is typical of oil-prone fields of this play, West Ranch lies landward of the depositional axis of the system, as delineated by quantitative facies maps of sand distribution (Galloway and others, 1982). The petroleum geology was described by Bauernschmidt (1944) soon after discovery of the field, and related data are contained in hearing files of the Oil and Gas Division of the Railroad Commission of Texas.

The main producing structure in West Ranch field is a simple dome (fig. 7). A small satellite dome lies to the southwest, but only the Ward, *Marginulina*, and Glasscock sands are productive at this subsidiary dome. Stratigraphic setting of the producing interval is illustrated by the regional cross section shown in figure 8. The thick

succession of blocky to upward-coarsening sand bodies of the middle and upper Frio shore-zone axis (wells 6 through 9) breaks up landward, and sand units are increasingly isolated by interbedded lagoonal or coastal plain mudstones (wells 2 through 5). Landward of well 2, which is the updip margin of the producing West Ranch dome, most of the individual sand bodies pinch out into the coastal plain and lagoonal facies. At the basinward fringe of the cross section, the shore-zone sand bodies are separated by and pinch out into marine shelf mudstones. The upper Frio shore-zone axis is centered along a major growth fault (developed primarily in the lower Frio) projected into the section between wells 11 and 12. Basinward of this axis, relations of the progradational shore-zone sand bodies and bounding mudstones define at least seven episodes (labeled A₁, A₂, B₁, and so on) of offlap and transgression. As is typical throughout the middle Coastal Plain, the Frio is here capped by a massive sand body called the Greta sand. The Greta consists of thick aggradational units that abruptly recede landward, reflecting the end of regional Frio continental margin offlap. The Greta is buried beneath marine shelf mudstones of the Anahuac Shale. Three such aggradational units, labeled E₁, E₂, and F, are also indicated on the cross section (fig. 8).

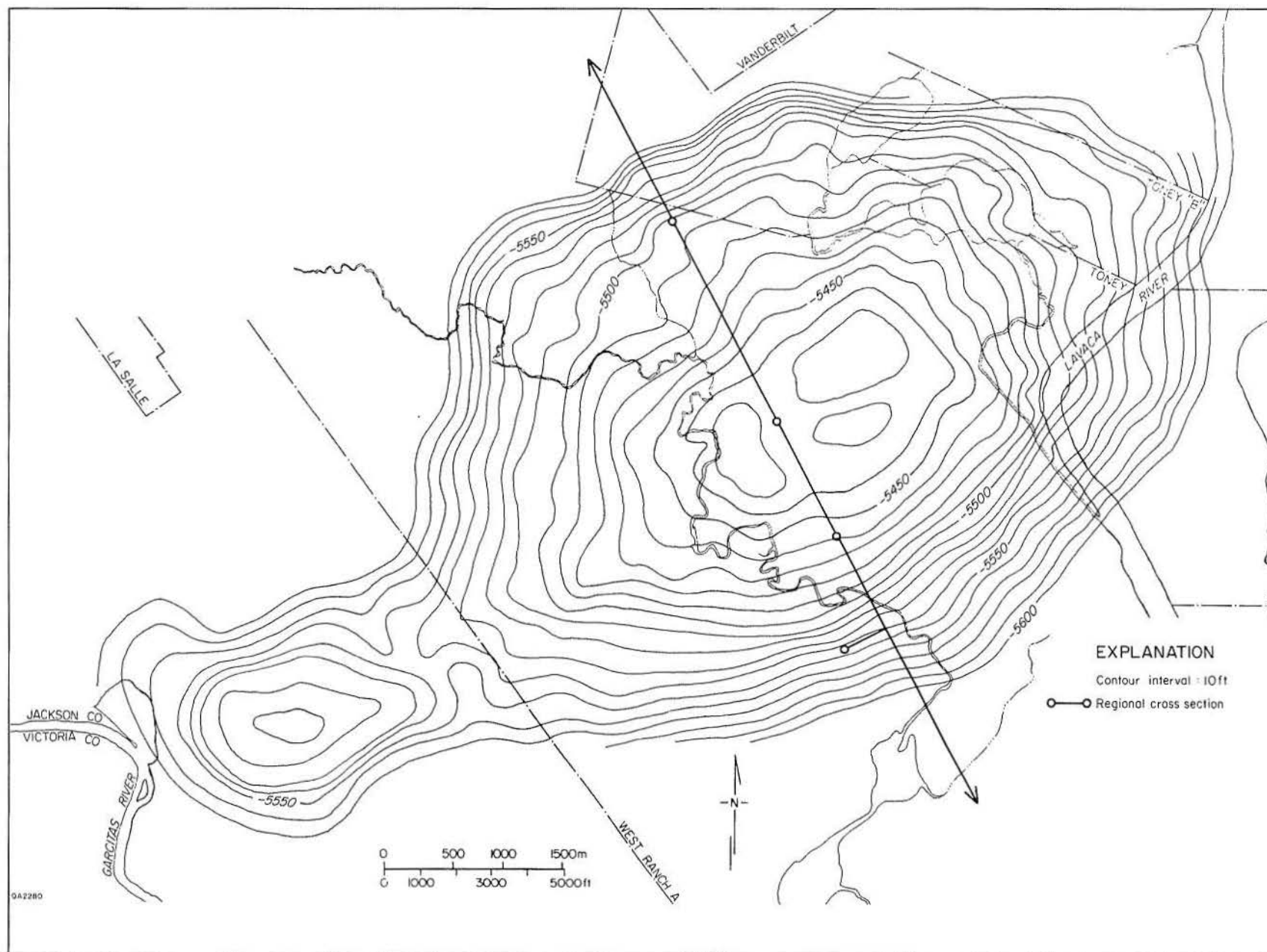


Figure 7. Structure-contour map of West Ranch field showing the simple domal anticline that creates the trap. Datum is the top of the Glasscock sand. Map courtesy of Mobil Producing, Texas and New Mexico.

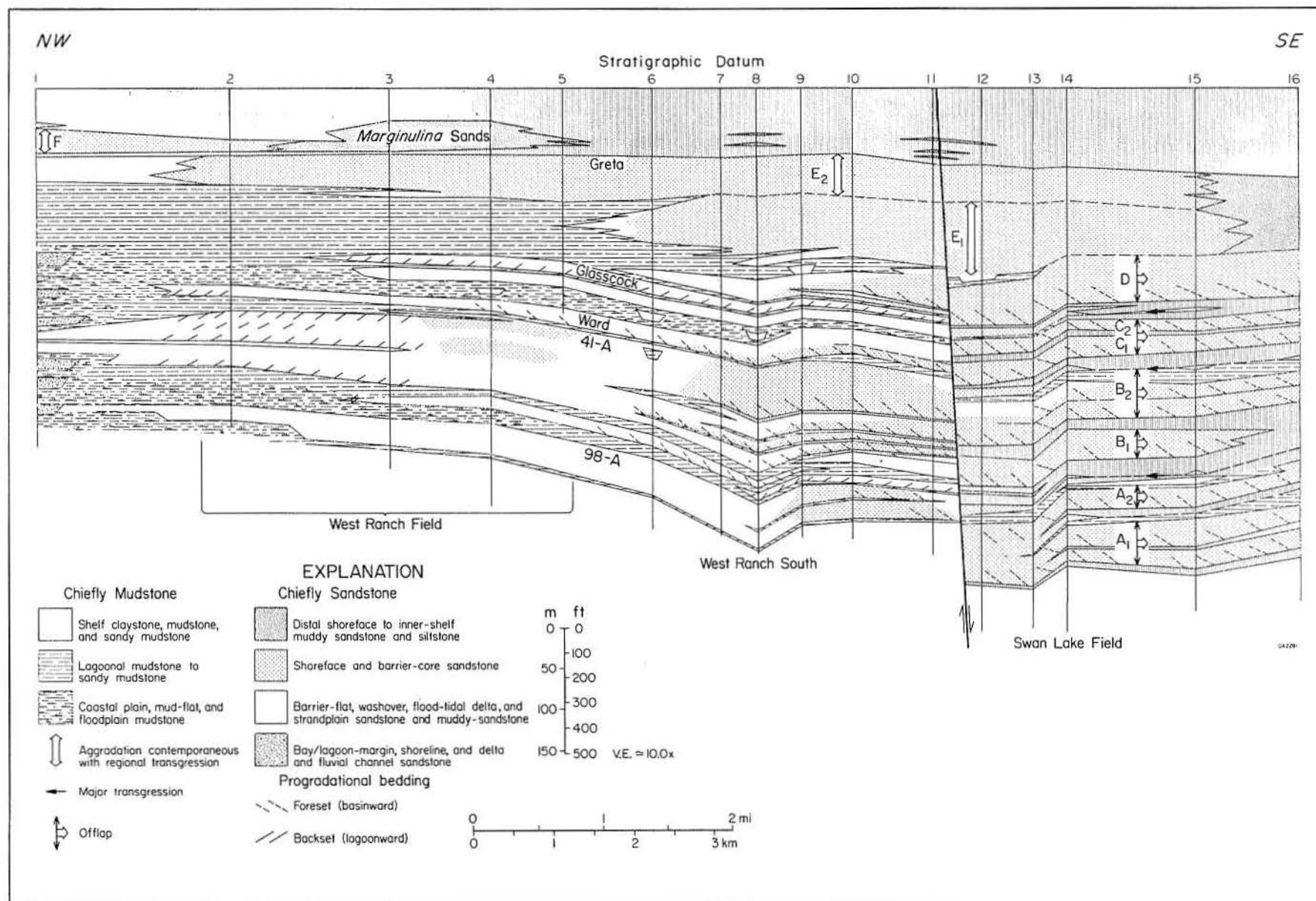


Figure 8. Dip-oriented regional cross section through West Ranch field. West Ranch field lies updip of the sand-rich axis of the Greta/Carancahua barrier/strandplain system. Stratigraphic relationships indicate six cycles of progradation or aggradation (labeled A through F) separated by transgressive marine shales. Main producing reservoirs in West Ranch field are labeled. For location of section see figure 7.

Five reservoirs have individually produced more than 10 million barrels of oil. In descending stratigraphic order they are the Greta, Glasscock, Ward, 41-A, and 98-A sands (fig. 8). Numerous additional sands in the upper Frio section have produced lesser amounts of oil or gas. The Greta reservoir, as described previously, is a massive, aggradational barrier sequence isolated landward by thick lagoonal mudstone and sealed by overlying shelf mudstone. Accumulation of distal shoreface and inner-shelf sands, the *Marginulina* sands, across the West Ranch dome resulted in a locally thin and poorly developed shale seal. The Glasscock, in contrast, is one of the most widespread reservoirs in the field. It is a particularly thin barrier-island sand body that was deposited during a local transgression terminating the "C" cycle of strandplain progradation (fig. 8). The 41-A reservoir is a moderately thick sand body that occurs at the top of the widespread sands of the "B" cycle and landward of the depositional axis of the cycle. Well-developed upward-coarsening sequences do not appear at the 41-A stratigraphic position for several miles farther basinward (well 11). Stratigraphic relationships suggest that much of the reservoir is overlain, and therefore sealed, by lagoonal mudstones deposited landward of a prograding barrier sand complex. The Ward and 98-A reservoirs are both landward parts of relatively thin progradational sand units. On the basis of their sheetlike geometry and regional facies relationships they are inferred to be strandplain deposits similar to those described by Tyler and Ambrose (in press).

The Greta, Glasscock, and 41-A zones are examples of barrier-bar reservoirs deposited in

aggradational, transgressive, and progradational stratigraphic settings, respectively. They exemplify the depositional architecture and productive attributes of barrier-island sand bodies deposited in the three key stratigraphic settings. Reservoir and fluid properties, production history, and geologic attributes of all three reservoirs are summarized in table 1. Together these three zones have produced nearly 200 million barrels of oil and 160 Bcf of gas. Each has experienced a somewhat different history of development following initial discovery and drilling. Pressure maintenance by infill or peripheral water injection, propane flooding, and waterflooding have been attempted; these techniques achieved varying degrees of technical success.

41-A Reservoir— A Progradational Barrier Sandstone

The 41-A reservoir is interpreted to be a simple barrier-island sand body comparable in scale and facies architecture to modern progradational barriers of the Texas Gulf Coast, such as Matagorda Island. Width of the sand body exceeds 5 mi (8 km) (fig. 8), but variation in vertical sequences suggests that it is a composite unit composed of at least two laterally equivalent, genetic barrier-island complexes. Thickness of the sand body ranges from 10 to 20 ft (3 to 6 m) along the updip (landward) margin of West Ranch field to more than 100 ft (30 m) near the fault shown in figure 8.

The reservoir is conventionally subdivided into three zones, (1) a discontinuous capping "stringer" that rarely exceeds a thickness of 10 ft (3 m), (2) a

Table 1. Characteristics of the Greta, Glasscock, and 41-A reservoirs, West Ranch field. Based on data in Atlas of Major Texas Oil Reservoirs (Galloway and others, 1983) and other sources. OWC = oil-water contact, GOC = gas-oil contact, GOR = gas-oil ratio, OIP = oil in place.

RESERVOIR PROPERTIES								
Reservoir	Disc. date	Avg. net oil pay (ft)	Avg. porosity (%)	Avg. permeability (md)	Initial water saturation (%)	Original OWC (ft)	Original GOC (ft)	Reservoir genesis
Greta	1938	35	31	1,000+	33	5,118	5,065	Aggradational barrier bar
Glasscock	1939	20	29	540	45	5,570	5,475	Transgressive barrier bar
41-A	1940	31	30	900	28	5,750	5,690	Progradational barrier bar

“main” zone that constitutes the body of the reservoir and contains most of the hydrocarbons, and (3) a “submain” sand, which is interpreted to be a genetically unrelated unit separated from the main sand by a thin poorly developed shelf mudstone. Both the main and stringer zones exhibit prominent depositional topography. As a result, the structure contoured on the top of the

41-A sand shows a complex morphology superimposed on the simple, first-order structural doming (fig. 9). Numerous curvilinear structural ridges and troughs transect the crest of the dome, reflecting a comparable ridge-and-swale depositional topography on top of the sand body. Differential relief between adjacent ridges and swales is as much as 20 ft (6 m).

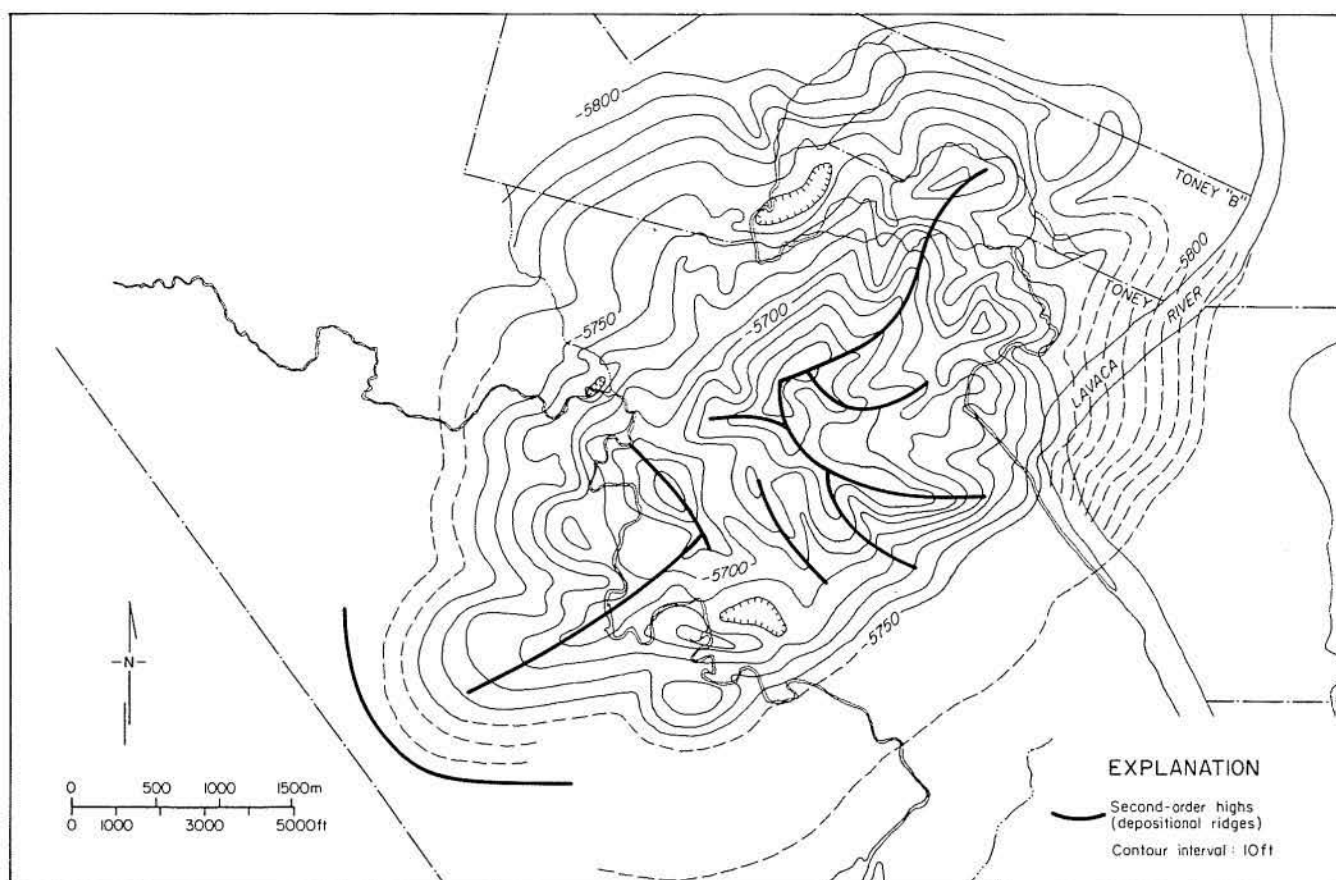


Figure 9. Structure-contour map of West Ranch field showing the combined domal structure and superimposed depositional topography of the 41-A reservoir, which is the datum. Map courtesy of Mobil Producing, Texas and New Mexico.

FLUID PROPERTIES					PRODUCTION HISTORY				
API gravity	Original GOR	Original oil viscosity (cp)	Temp. (°F)	Drive mechanism	Cumulative production (MMbbl oil)	Estimated OIP (MMbbl)	Est. ult. recov. efficiency (%)	Production technology	
24°	325	1.32	160	Water drive	76.5	Plus approximately 42 MMbbl produced before individual reservoirs separated in 1950	223	42	Pressure maintenance
31°	440	0.69	168	Gas-cap expansion and water drive	38.2		127	38	GOC peripheral waterflood
32°	521	0.65	171	Water drive	78.0		149	52	Pressure maintenance

An isopach map of the 41-A main and genetically associated stringer sand zones (fig. 10) shows similar curvilinear trends. Across the northeastern and central parts of the field, strongly dip-oriented contour trends prevail. The sand body is also thickest there; contour values commonly exceed 70 ft (21 m). To the southwest, the sand body is thinner, typically ranging

between 30 and 50 ft (9 and 15 m) thick, and displays prominent strike-oriented contours. The sand body thins and orientations become complex along the northwestern (or landward) margin of the field.

A map of spontaneous potential (SP) log patterns (fig. 11) shows that six common patterns, or log facies, occur within the field area. Blocky

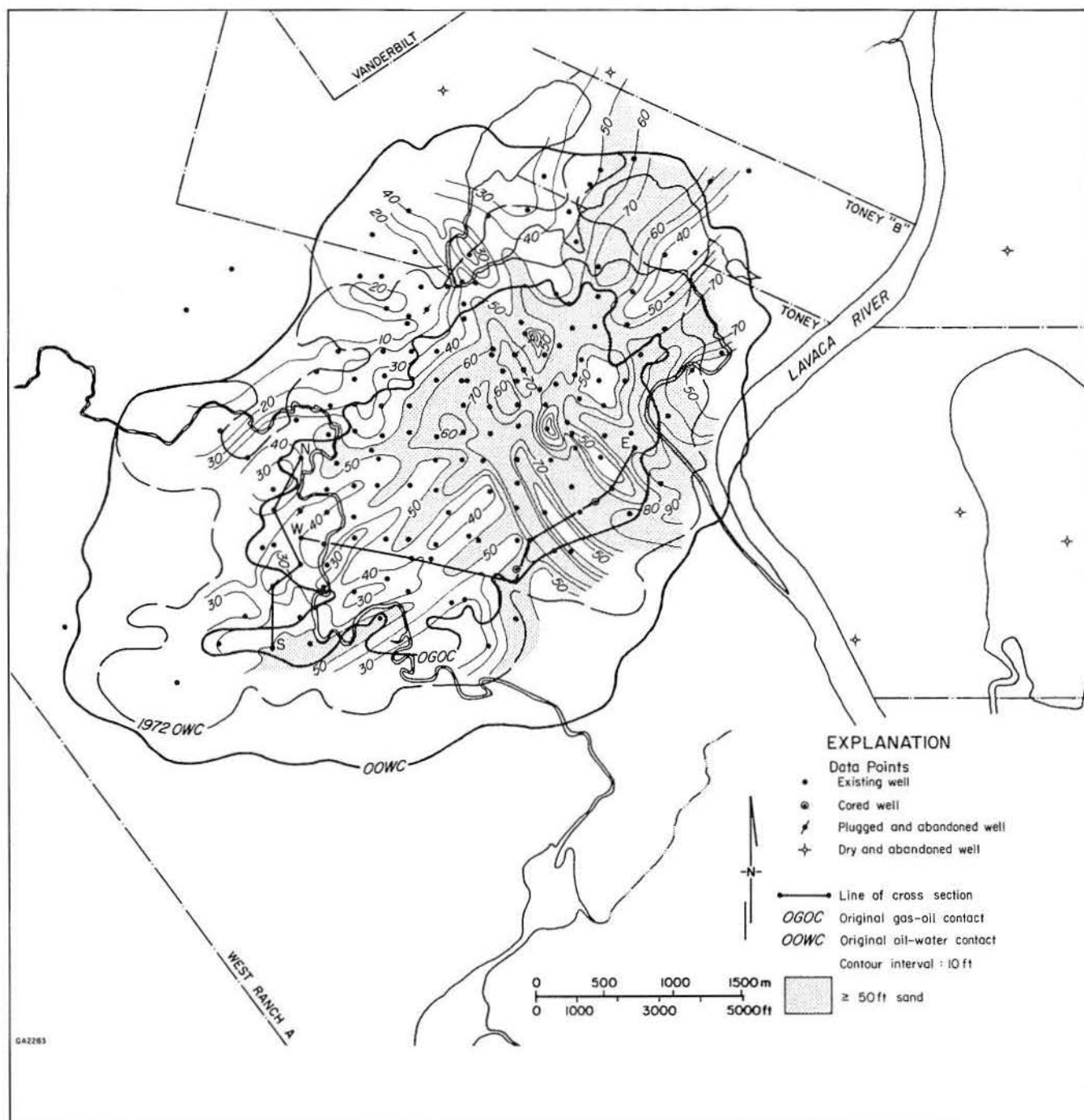


Figure 10. Net-sand isolith map of the 41-A main and the genetically associated stringer reservoir.

and blocky-with-shoulder patterns (motif A₁, fig. 11) characterize the area of thickest 41-A sand in the east-central field area. These patterns closely resemble the inlet SP log pattern (fig. 5). Sharp-based deflections having an upward gradation (motif A₂, fig. 11) are grouped along the southern margin of the field. Blocky deflections having a thin basal transition zone (motif B)

typify the south-central part of the field, in the area of prominent strike-parallel contours. Increasingly serrate SP patterns (types C, D, and E) cluster around the updip fringe of the field, in the area of sand thinning and irregular contours. The areal distribution and serrate nature of these types closely resemble flood-tidal delta and back-barrier SP logs from Galveston Island (fig. 5).

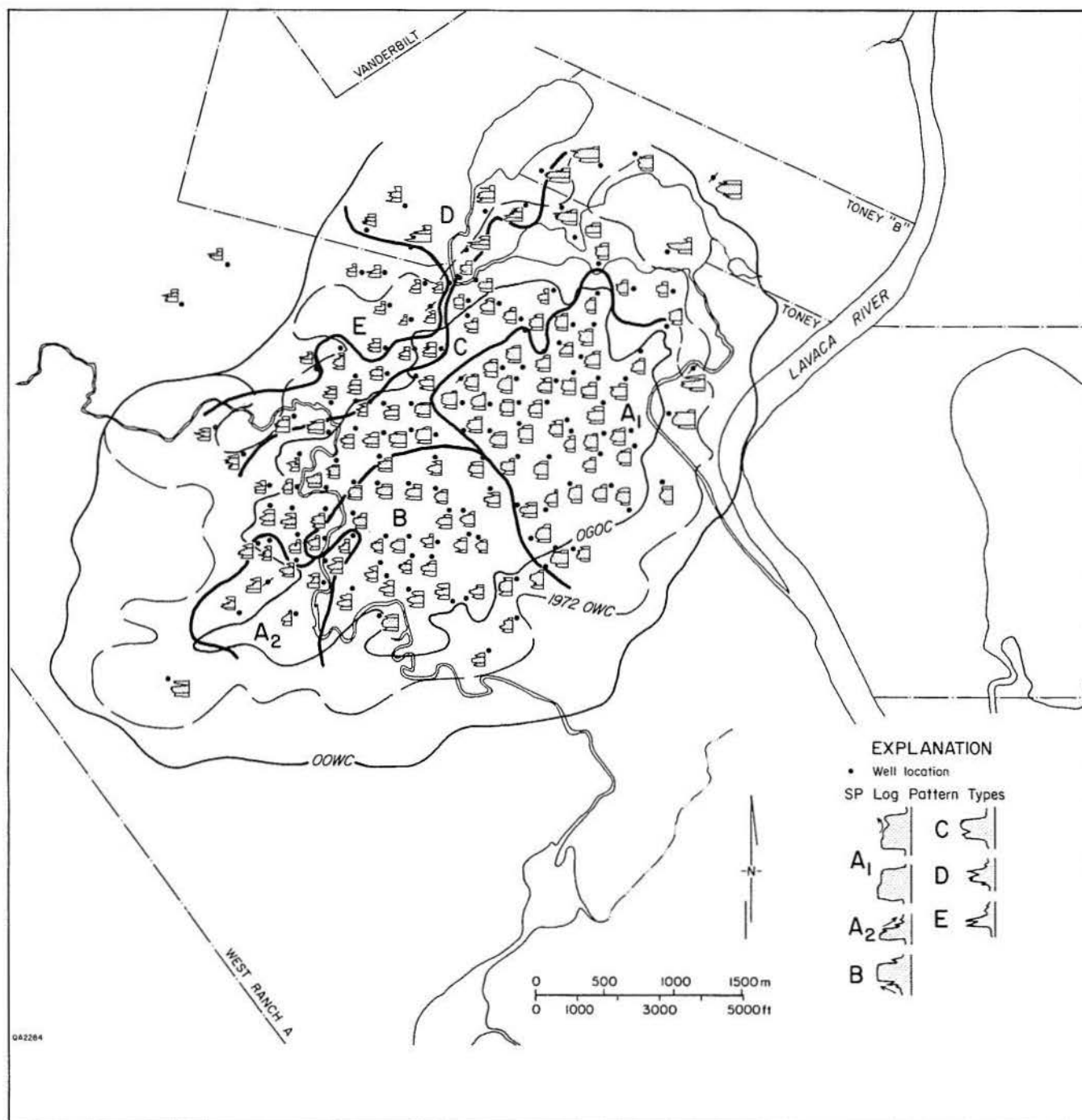


Figure 11. Map of SP log patterns of the 41-A sand.

Component Barrier-Island Facies

The regional setting, detailed sand-body geometry, and nature and distribution of vertical textural sequences as interpreted from SP logs reveal the presence of several component facies of barrier islands within the 41-A sand in West Ranch field (fig. 12). Principal facies elements include barrier core and underlying thin shoreface, tidal-inlet fill, flood-tidal delta, and back-barrier/lagoon transition (fig. 12). Geometry and distribution of facies elements closely parallel those observed at the northern end of Matagorda Island and adjacent Pass Cavallo, which is a major tidal inlet (Wilkinson, 1975).

Barrier-Core Facies

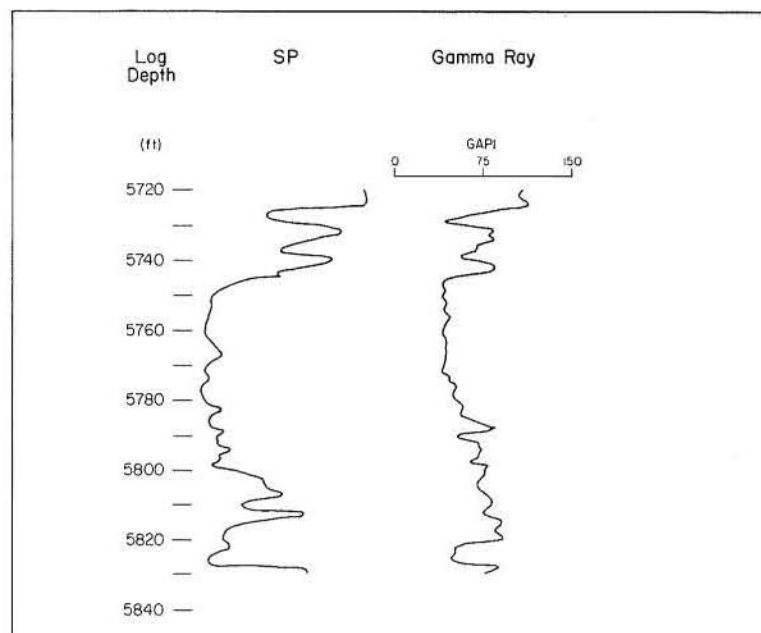
The barrier-core facies is characterized by a strike-parallel depositional trend (expressed by the strike-parallel grain of isolith contours), an average thickness of 30 to 40 ft (9 to 12 m), and a thin basal transition zone into underlying muddy sand and mud of shelf and distal shoreface origin. The gamma-ray log reflects this basal transition with greater fidelity than does the SP log (fig. 13). Detailed core and log data from a recently drilled well allow more thorough description of this facies (fig. 13). The barrier-core facies consists of fine, well-sorted to moderately well sorted sand. Sorting improves slightly upward, but the narrow range of grain size shows little evidence of an upward-coarsening gradient within the middle and upper sand body. Likewise, neither core-plug porosity nor log porosity shows a clear vertical trend; porosity exceeds 30 percent throughout the sand body. In contrast, permeability is highest at the top of the sand body (beach), is high within the middle, massive part of the sequence, and appears to decrease toward the base, probably because of increasing but minor mud content.

Inlet-Fill Facies

Two inlet fills are interpreted to transect the 41-A barrier-core facies in the field area (fig. 12). The major inlet fill, which lies in the northeast quadrant of the field, is characterized by unusually thick sand, a prominent dip-oriented pattern of isolith contours, and sharp-based, blocky log patterns. A blocky SP response that exhibits an abrupt basal deflection, a gentle decline in the middle, and a maximum deflection (forming a "shoulder") on top is characteristic of inlet fill. The sequence reflects the basal scour,

upward-fining inlet-fill sequence that is capped by a spit platform and beach (Heron and others, 1984). A localized inlet fill lies at the southwestern margin of the field. This minor inlet unit may consist, in the field area, primarily of the landward tidal channels radiating from the inlet of a slightly younger downdip barrier, or it may be a temporary cut through the 41-A barrier island. Both inlet fills are capped along their downdip segments by the laterally accreting spit-platform sands—the shoulders at the top of many of the SP logs. The minor inlet fill, however, contains a partial plug of finer muddy sediment, resulting in the common upward-fining log response. The major inlet-fill unit typically is massive sand, although isolated and anomalously low sand thickness values (fig. 10) suggest local preservation of a muddy plug.

A few cores and several modern log suites provide information about the internal composition and reservoir properties of the inlet-fill facies (fig. 14). Gamma-ray and SP logs show a similar response. Sands are fine to very fine grained and well to moderately well sorted, and vertical grain-size gradients are subdued. Coarsest sand lies at the base of the inlet fill. Variations in texture and in log response appear to be mainly a product of variation in dispersed clay content. The capping spit sands contain the least admixed clay. Although sedimentary structures are difficult to discern in the unconsolidated sands, crossbedding



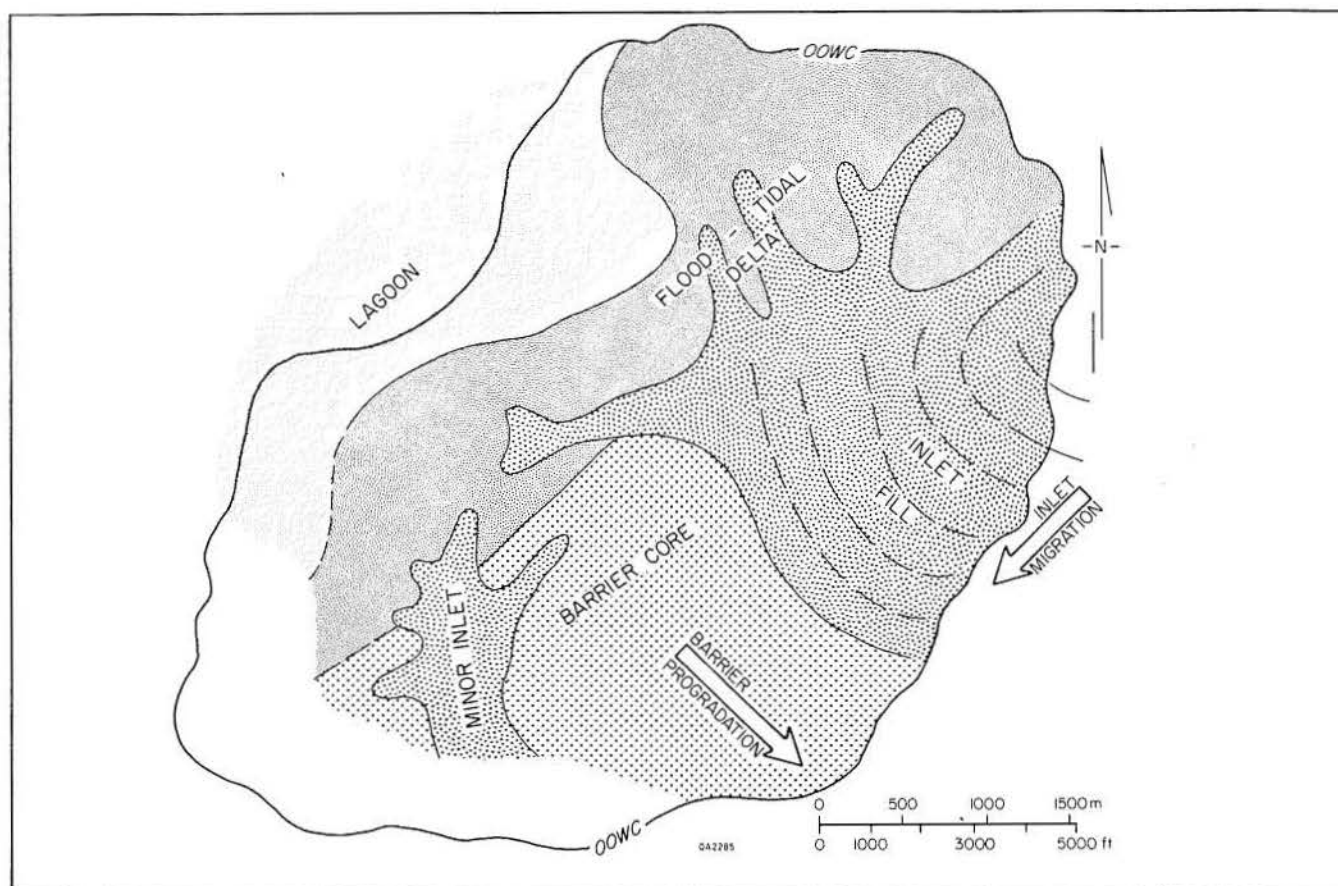


Figure 12. Interpreted depositional elements of the 41-A sand.

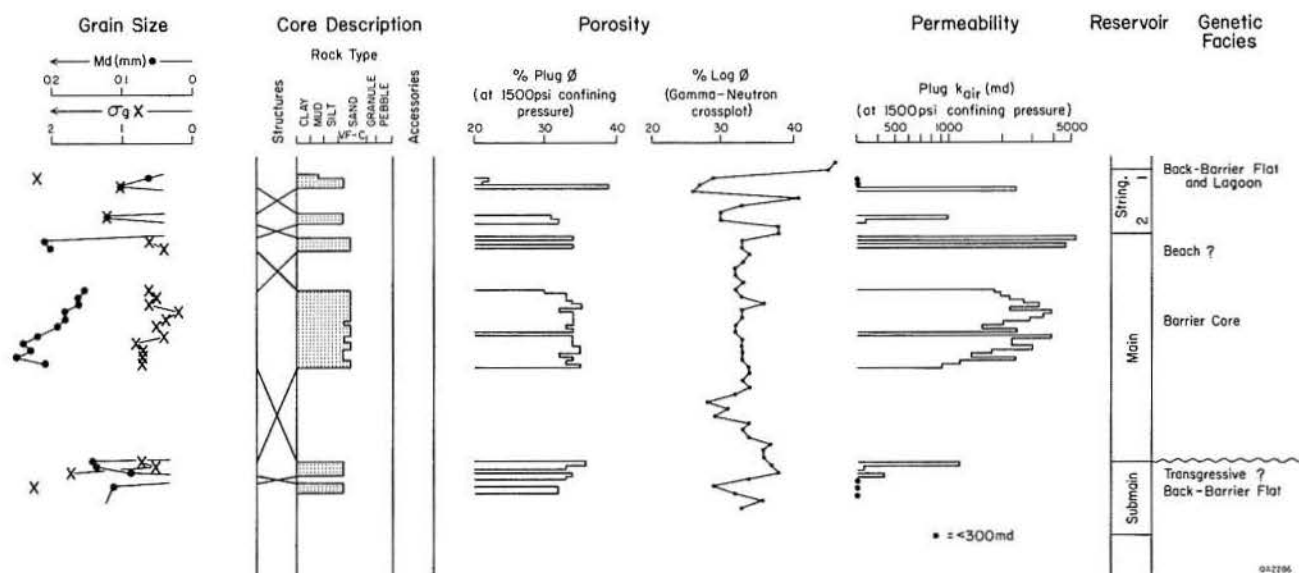


Figure 13. Log response, texture, internal features, and petrophysical properties of the barrier-core facies of the 41-A reservoir, well A-493.

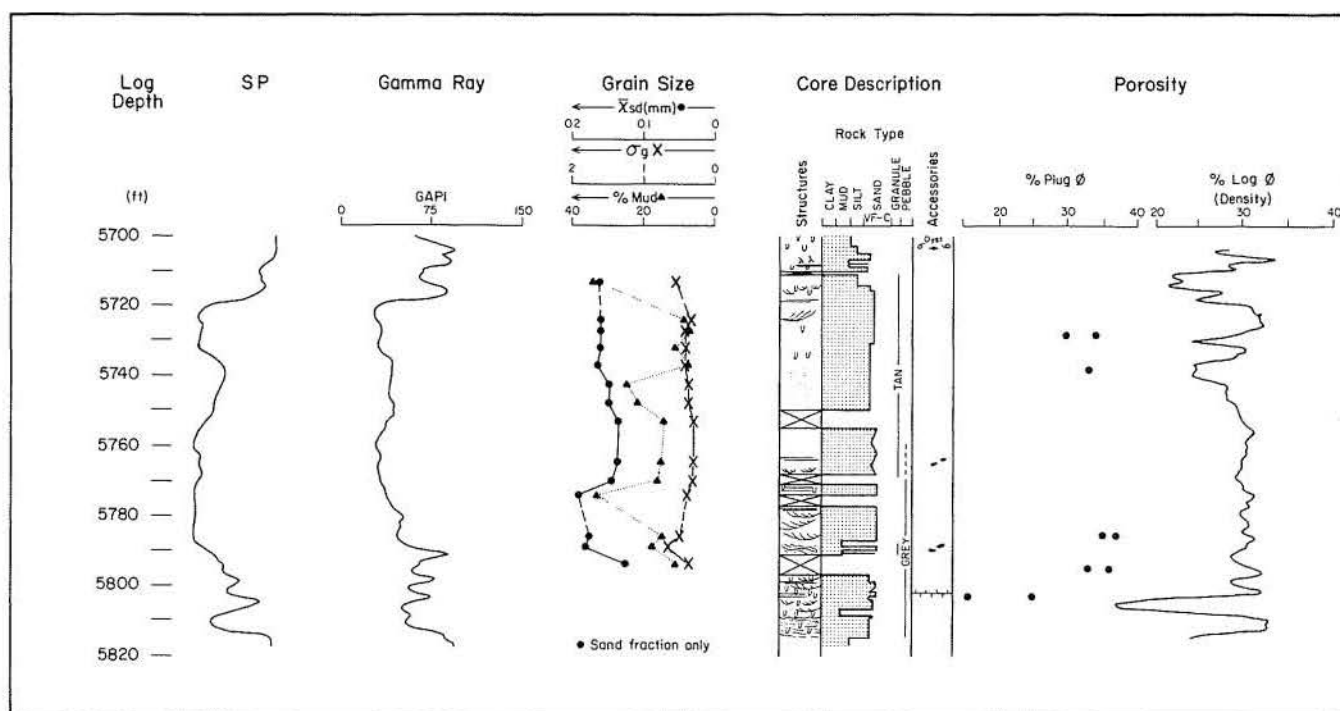


Figure 14. Log response, texture, internal features, and petrophysical properties of the inlet-fill facies, 41-A reservoir, well A-496.

is apparent at the base of the inlet fill. Most of the fill consists of homogeneous, faintly bioturbated sand. Faint planar lamination and cross-lamination occur within the capping spit platform sequence. Overlying stringer sands are bioturbated and contain oystershell and plant debris. In this and other cores of Frio sands in West Ranch field, color seems correlative with inferred environment—tans with shallow-water to subaerial settings and gray or olive with deeper water or lagoonal settings. Porosity appears to be higher (30 to 35 percent) at the base and top of the inlet fill. Permeability distribution shows similar patterns (see also plate 1).

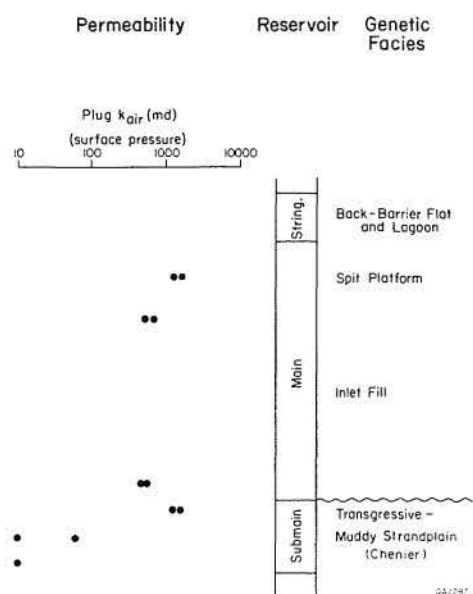
Lateral Facies Relationships

Plate 1 shows a strike (E-W) section through the major inlet-fill and barrier-core facies elements. The 41-A sand inlet fill is comparatively thick, ranging from 60 to 70 ft (18 to 21 m). Electric log profiles suggest a mix of both the simple upward-fining pattern (well A-423) and the upward-fining with capping shoulder pattern (wells A-424, A-496) typical of the inlet-fill sequence. Core plug and log-derived porosity and permeability profiles show that reservoir quality, notably permeability, commonly parallels the log profile. The spit-

platform shoulder reflects a zone of enhanced permeability and porosity. Zones of high permeability also occur sporadically within the otherwise massive inlet fill (well A-423, 5,743 to 5,752 ft, for example). Plug permeability within the massive inlet fill commonly exceeds 1 D.

The abrupt erosional margin of the inlet fill lies between wells A-423 and A-427. To the west, barrier-core sands are 35 to 50 ft (10 to 15 m) thick. Best reservoir quality occurs at the top of the sequence (wells A-427 and A-428, for example). The preserved shoreface facies at the base of the barrier core is thin or poorly developed. The lower 20 ft (6 m) of sand has erratic permeability values that rarely exceed 1 D, suggestive of interbedding in texturally heterogeneous layers. Contrast in lateral stratigraphic position of zones of maximum permeability between the inlet-fill and barrier-core facies is dramatically shown by the juxtaposition of wells A-423 and A-427 (pl. 1).

Facies and reservoir-quality changes along the axis of an inlet and associated tidal channel are illustrated by a dip-oriented cross section along the minor inlet fill (pl. 1). A typical although somewhat thin inlet-fill sequence having a thin, capping spit-platform shoulder is penetrated by well A-476 at the downdip end of the cross section. Landward, the inlet fill is in part a muddy plug. An



analogous, partly plugged tidal-channel fill, Packery Channel, described by Morton and McGowen (1980), cuts across Mustang Island. Depth of tidal-channel scour decreases lagoonward, and a basal, upward-coarsening flood-tidal delta sequence underlies the channel fill in wells A-196 and A-376. The limited data suggest that permeability is greatest within the tidal-channel sand, intermediate in the flood-tidal delta sands, and poorest in the muddy channel plug. The most updip well (A-189) displays interbedded muddy sand and mudstone typical of the barrier/lagoon transition. In summary, the cross section reveals two general trends. First, both thickness and reservoir quality of the barrier facies assemblage decrease toward the lagoon. Second, the upper parts of tidal channels, which transect the back-barrier and tidal-delta facies, are locally filled by muddy plugs that may partly isolate the upper part of the reservoir.

Overview of Reservoir Facies Heterogeneity

Detailed facies analysis shows that the 41-A reservoir consists of five major facies elements within the approximately 6-mi² (15-km²) areal

extent of the field: (1) major inlet fill; (2) minor inlet and tidal-channel fill; (3) barrier core; (4) flood-tidal delta; and (5) back-barrier/lagoon transition.

On the basis of knowledge of modern barrier-island depositional architecture (fig. 3), the internal bedding geometry of the 41-A reservoir can also be inferred to differ from facies to facies. The barrier core most likely consists of gently seaward-dipping, imbricate tabular beds, exhibiting updip and downdip transitional margins. In contrast, inlet fill probably contains lateral-accretion bedding, produced in part by spit-platform growth onto the updip flank of the inlet, and crosscutting internal scour fills, reflecting cut-and-fill processes within the channel. Tidal-delta and transitional back-barrier sands contain a complex suite of tabular beds and crosscutting lenses. Boundaries of internal barrier facies elements are both abrupt and transitional.

Permeability Distribution

Permeability distribution reflects the facies distribution and varies internally within each facies. A map of average permeability of the 41-A main reservoir (fig. 15), based on data from wells adequately sampled by core plugs, supports the inference of lateral variation of reservoir quality made on the basis of detailed core and log studies. Greatest permeability values exist in the barrier-core facies and at the top of the sand body. Average values are as much as several darcys high, and isopermeability contours parallel the strike orientation of the barrier core. Inlet fills are also quite permeable, but maximum permeability occurs toward the base, as local pockets within the inlet fill, and in the spit-platform cap at the top of the sand body. Average permeability in inlet-fill units rarely exceeds 1 D, and trends are dip oriented. In back-barrier facies, including tidal-channel, flood-tidal-delta, and transitional sands, permeability is reduced and distribution is more erratic and heterogeneous.

Weber and others (1978) found that, in the hydrocarbon-saturated zone, measured formation resistivity could be used to derive a semi-quantitative approximation of reservoir permeability. A correlation between deep resistivity and permeability is suggested by the similarity of the profiles shown in plate 1 (compare wells A-423 and A-427, for example). A logarithmic plot of permeability against deep resistivity based on core plug measurements and electric logs from six wells

in the 41-A reservoir is shown in figure 16. Three wells, A-427, A-375, and A-376, penetrate the barrier-core facies; the other wells, A-420, A-423, and A-424, penetrate the inlet-fill facies. The two facies show little difference in general trend on the plot. However, a well-correlated trend between permeability and deep resistivity exists for samples having permeabilities greater than 1 D. For permeabilities of less than 1 D, deep resistivity

is usually less than 4 ohm-m but is otherwise insensitive to reservoir permeability.

Regression analysis of log k against log resistivity for all the data points plotted gave a correlation coefficient of nearly 0.6. The plot reinforces the observed correlation of highest permeabilities with barrier-core facies; thus, resistivity could be used to guide interpretation of three-dimensional permeability distribution.

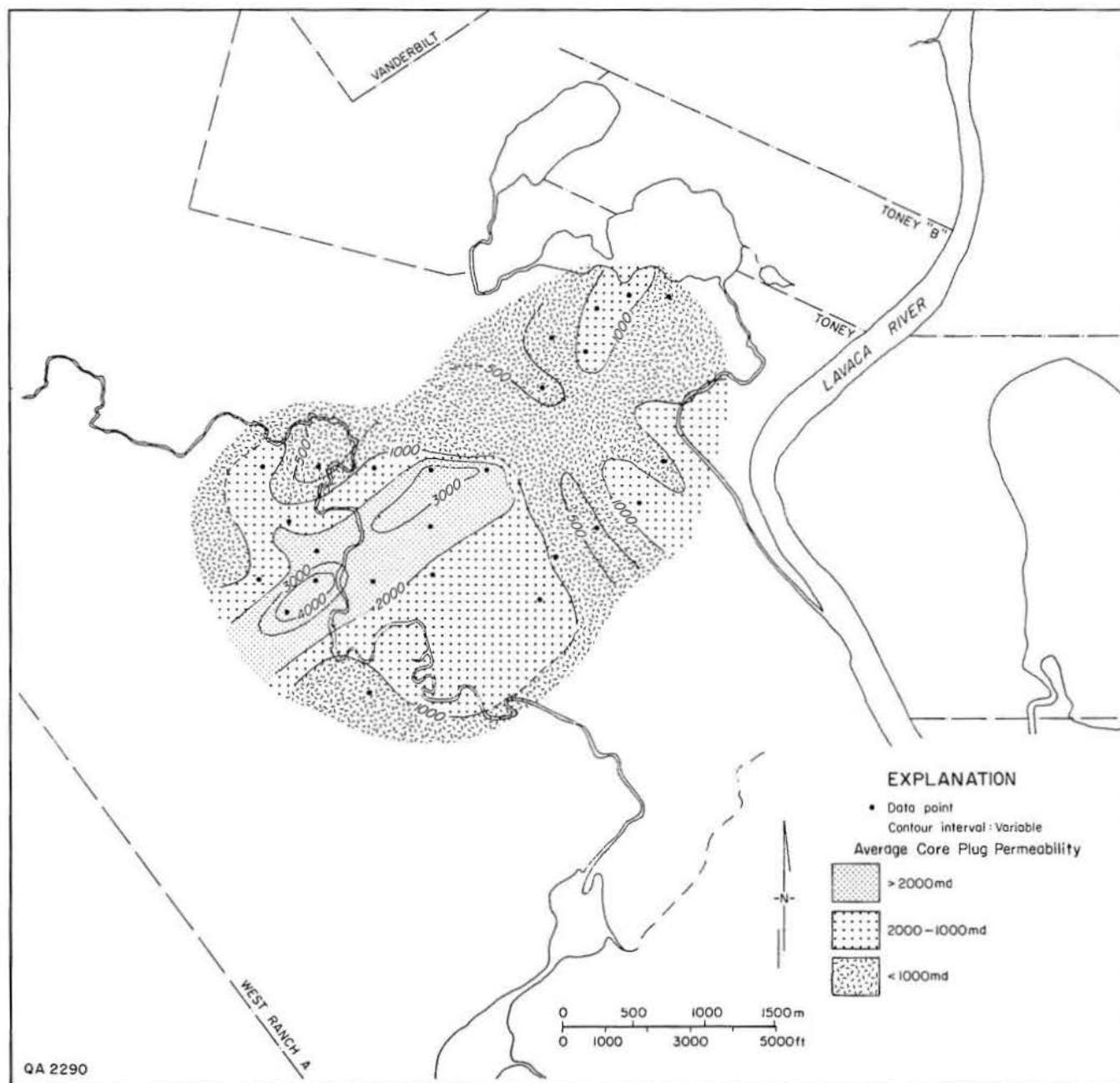


Figure 15. Map of average 41-A reservoir permeability. Control points are cored wells for which representative suites of core-plug permeabilities have been measured. Permeability distribution reflects the genetic facies elements of the reservoir.

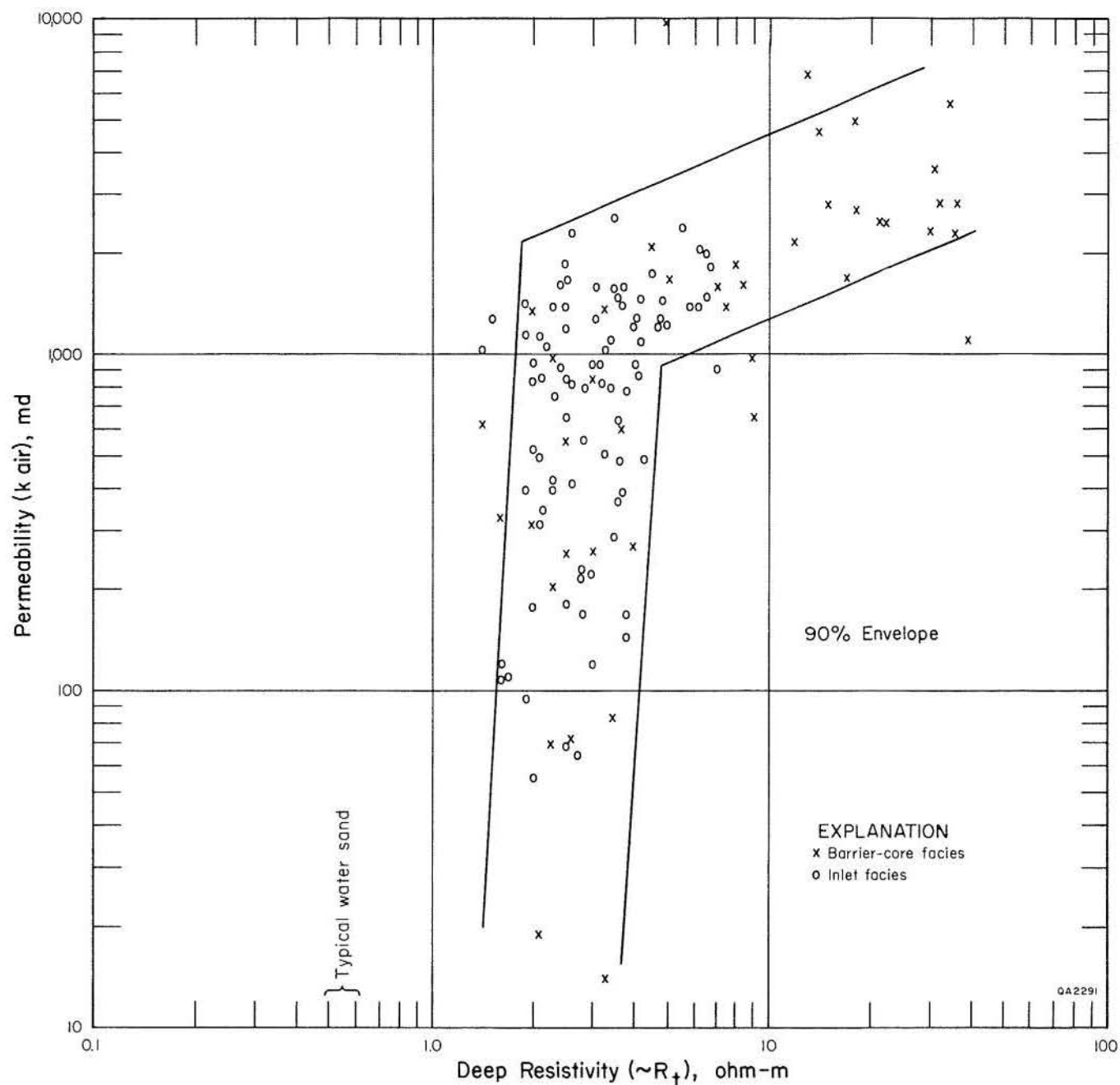


Figure 16. Cross plot of measured core-plug permeability (k) and log-derived deep resistivity (R_d) within the hydrocarbon-saturated zone of the 41-A reservoir.

Resistivity Patterns and Hydrocarbon Distribution

In formations where invasion of mud filtrate is minimal, measurements of deep resistivity may be used to calculate water saturation (S_w), provided that porosity is known or can be approximated. Comparison of deep and shallow resistivity curves of the various reservoirs in West Ranch field

indicates that deep resistivity closely approximates true resistivity. The limited range of porosity values indicated by log and core measurements simplifies generalized analysis of the spatial distribution of hydrocarbon saturation within the 41-A reservoir. The wide range of measured resistivities does not visually correlate with variations in porosity or with type of hydrocarbon (pl. 1). Furthermore, within the

hydrocarbon-saturated zone above the oil-water contact, irreducible S_w has been shown to be related to reservoir quality (permeability) in the Gulf Coast by empirical equations such as those formulated by Timur and Coates and by Dumanoir (Schlumberger, 1974, p. 38). Thus, analysis of resistivity distribution should delineate reservoir compartments distinguished by variations in S_w . Variable shale content will also affect the calculated S_w , but test calculations show that within a range of 0 to 20 percent shale (Vsh), estimated water saturation is changed by about 25 percent. This range is small compared with the wide range of water saturations indicated by varying resistivity.

Resistivity log patterns (within the structurally highest portion of the reservoir where the total

41-A main sand is hydrocarbon saturated) show a more diverse suite of motifs (fig. 17) than do the SP curves. Generally similar resistivity logs can be grouped into five motifs. These motifs show spatial distributions comparable to those of the genetic facies composing the 41-A reservoir. The barrier-core facies is characterized by a single, extremely high resistivity deflection, typically at the top of the main sand. In contrast, inlet fill displays a more diverse suite of resistivity motifs. Upward-increasing, upward-decreasing, and symmetrical deflections (log patterns IIa, b, and c) occur in dip-oriented trains (fig. 17) paralleling the dip orientation of isolith contours (fig. 10). Isolated wells within the inlet-fill facies show suppressed resistivity deflections (log pattern III). The back barrier and tidal delta are typified by

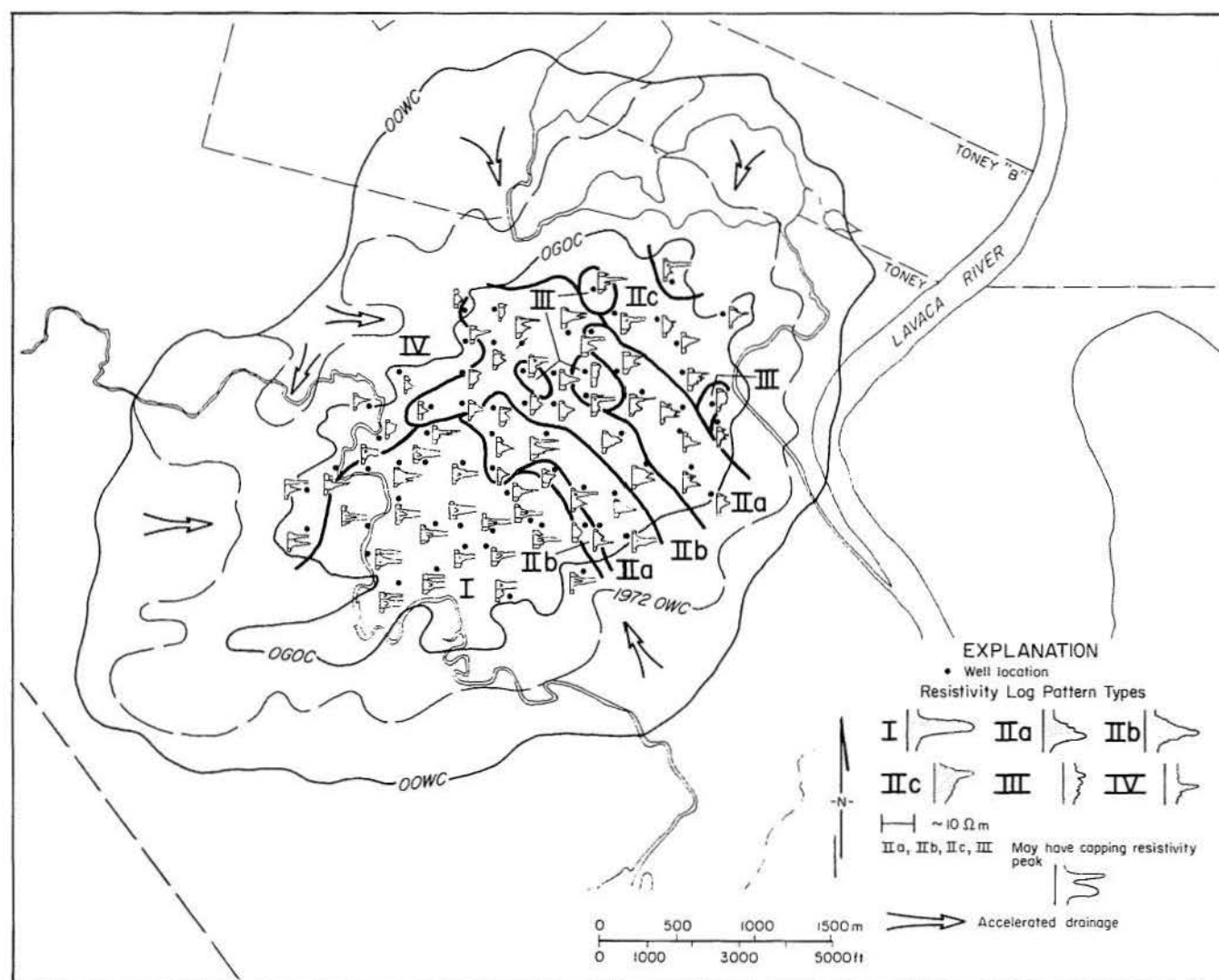


Figure 17. Deep-resistivity log patterns of the hydrocarbon-saturated portion of the 41-A reservoir. Four major motifs are defined.

sharp, thin, spikey (log pattern IV) or suppressed symmetrical (pattern IIb) deflections.

If measured deep resistivity closely approximates true resistivity and thus provides a semi-quantitative measurement of water saturation, then log-profile cross sections, such as those in plate 2, panel 1, should also show the three-dimensional hydrocarbon distribution within the reservoir. Immediately apparent is the relative continuity of the high-resistivity zone at the top of the barrier-core facies. In contrast, the inlet fill is characterized by discontinuity of resistivity zones in both dip and strike directions. The dip section across the barrier core (cross section E-F, pl. 2, panel 1) reveals the expected seaward imbrication of individual saturation compartments. Two prominent units, each a few thousand feet wide, occur within the saturated zone. The inlet fill is characterized by numerous discontinuous zones having low water saturation suspended within and capping an inlet-fill matrix containing average ($S_w = 29$ percent) to above-average water saturations. Wells A-350, A-411, and A-218 in cross section C-D, for example, show prominent zones having extremely high resistivity and a calculated hydrocarbon saturation that corre-

sponds to that of the highly permeable spit-platform sands capping the inlet fill. Comparison of dip and strike sections shows that well-to-well discontinuities of the high-resistivity zones are greatest in the strike direction, across the grain of the inlet-fill facies.

Interpretive contouring of resistivity zones (fig. 17) based on the facies model reveals the internal complexity of the 41-A reservoir. Within the larger depositional mosaic of the barrier-bar sand body and its component facies (fig. 3), the internal architecture of each facies results in the preferential distribution of hydrocarbons as a series of relatively rich zones enmeshed within less rich portions of the reservoir. Thus, saturation distribution, as expressed by variation in measured resistivity, provides the most detailed view of the internal building blocks of the reservoir sand body. These facies building blocks are small but similar in scale to their counterparts in modern barriers such as Matagorda Island. Geometry and areal extent of individual reservoir blocks, or saturation compartments, may be compared to the typical spacing of development wells (20 acres), and simple terms such as sheet, tab, pod, or channel can be used to describe them (fig. 18).

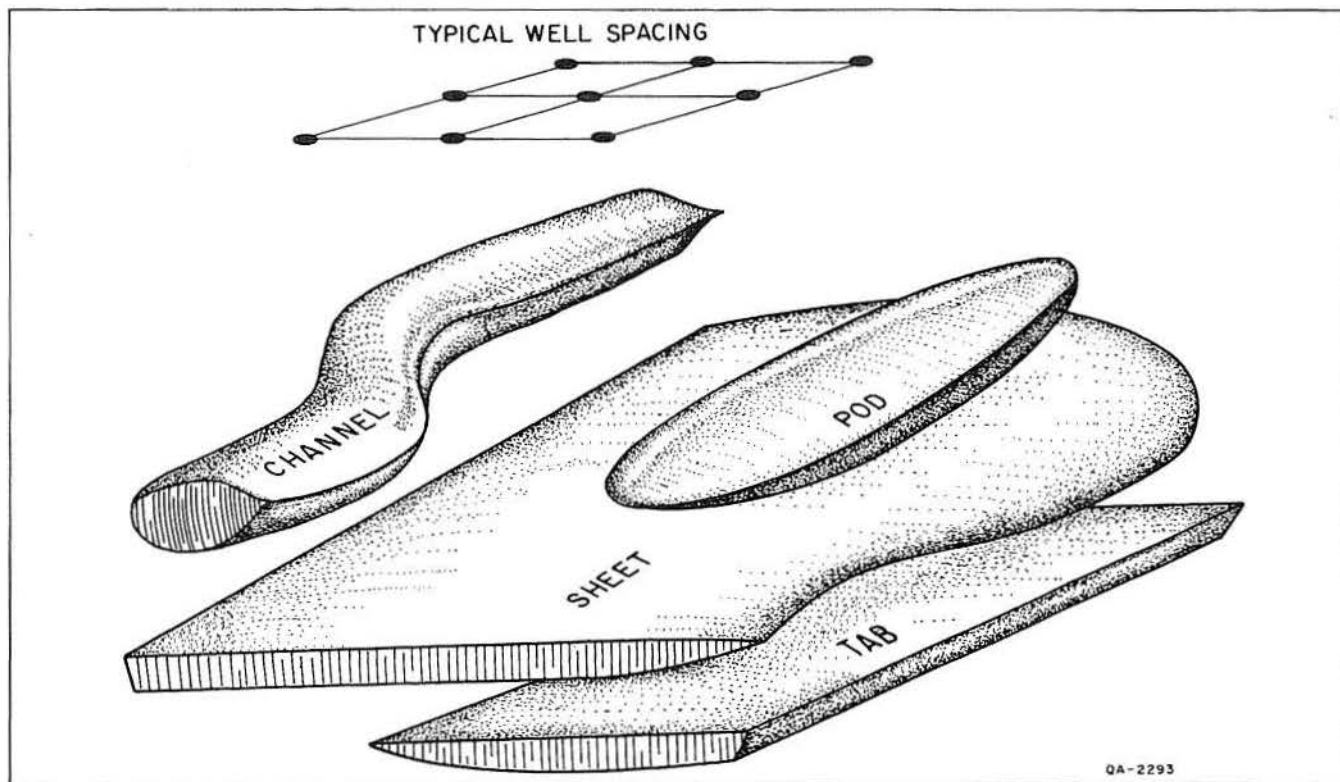


Figure 18. Geometries of resistivity (saturation) compartments. Terms are scaled to indicate continuity relative to conventional 20-acre well spacing of oil fields.

Panel 2 of plate 2 illustrates three of the resistivity cross sections redrawn to emphasize the internal compartmentalization of the sand body into numerous saturation lenses, pods, sheets, and tabs. Boundaries between saturation compartments, particularly where abrupt or where separating vertically contrasting saturation profiles, are likely to be flow boundaries or discontinuities. Conversely, flow of hydrocarbons within the same compartment is likely to be easier than flow across compartments. The combination of detailed facies analysis, using conventional SP log facies and isolith description, with analysis of saturation distribution provides a more complete picture of internal reservoir properties than is generally attempted or possible using conventional log or core analysis.

Correlation of saturation compartments with depositional facies should be mentioned. The 41-A reservoir sands reveal a variety of diagenetic features, including well-developed diagenetic clay coats and pore-fill and leached feldspar grains. Clay distribution and type, as well as relative abundances of microporosity, primary intergranular porosity, and secondary leached porosity, may influence residual water saturation (Pittman, 1979). If diagenetic facies are randomly

distributed within the depositional facies, use of environmental interpretation and mapping for projecting reservoir properties would be severely hampered. However, diagenetic patterns commonly reflect primary depositional facies, and many of the diagenetic features, such as clay coats seen in the 41-A reservoir, appear to be syngenetic and thus closely facies related. In the Frio barrier/strandplain reservoirs, diagenesis may accentuate rather than obscure differences in reservoir quality among various depositional facies.

Drainage History

The overall high permeability and porosity and efficient water drive of the 41-A reservoir combine to produce an excellent projected recovery of 55 percent of the oil in place. Nonetheless, even within the superficially homogeneous main zone, drainage has not proceeded uniformly. Advance of the oil-water contact has been irregular (fig. 10), particularly along the updip margin of the field in the back-barrier facies. A series of well tests revealed a similarly irregular distribution of water cuts and gas-oil ratios within the main zone (fig. 19). Prominent in figure 19 is the anoma-

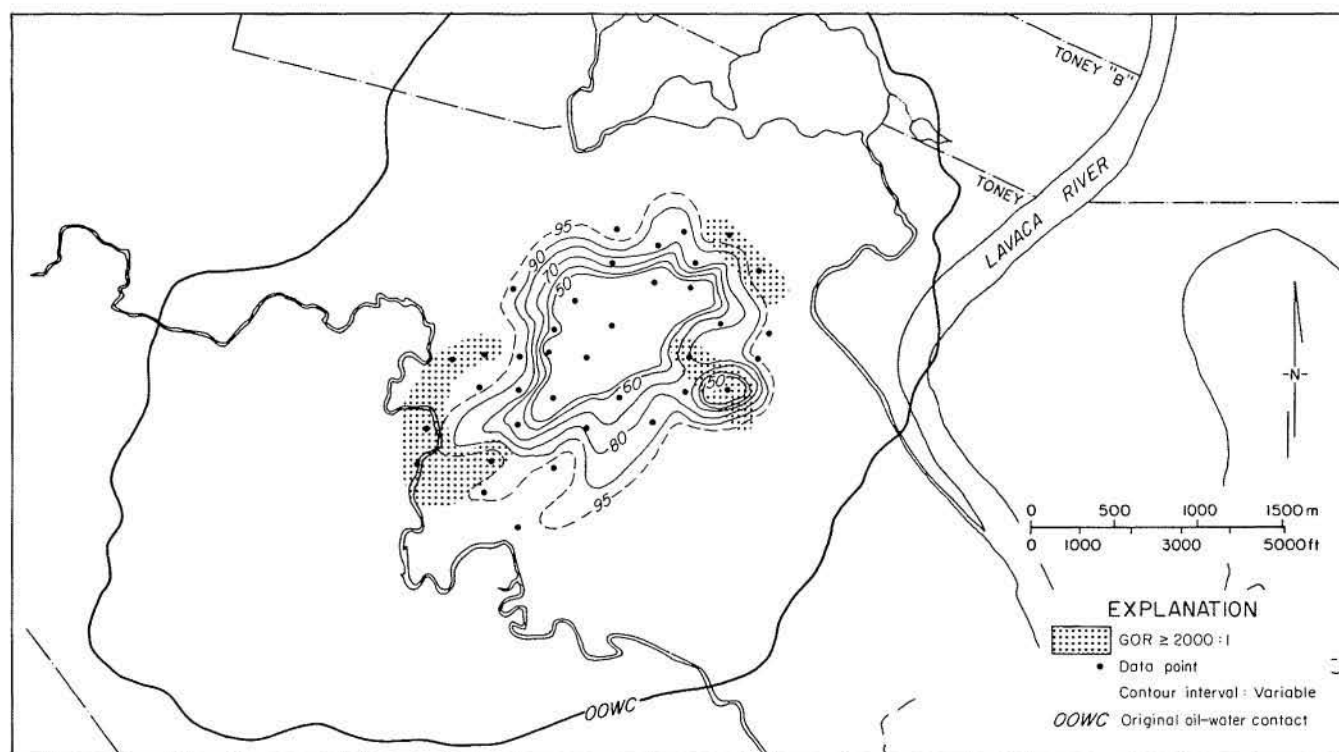


Figure 19. Water-cut distribution in test wells during latter stages of depletion of the 41-A main reservoir. Well tests were completed within a two-month period. Anomalously high gas-oil ratios are also shown.

lously low water cut exhibited by a well penetrating the inlet-fill along the downdip margin of the field. Anomalous drainage histories of individual wells or small groups of wells provide the most direct evidence that facies-controlled variation of reservoir properties and compartmentalization influence drainage of hydrocarbons. The anomalous well may tap an isolated reservoir pod within a specific inlet-channel unit. Drainage of such a pod by a single well may be inefficient, and infill drilling may be justified. Thorough analysis of drainage anomalies requires knowledge of perforation intervals in the test wells.

Accurate, three-dimensional description of reservoir properties and potential flow boundaries or favored trends, as well as of residual hydrocarbon saturation, are necessary preludes to accurate reservoir simulation and tertiary recovery processes. Semiquantitative description of initial saturation, reservoir quality, and facies compartmentalization, by use of the older electrical logs available from nearly all wells, allows extrapolation of parameters beyond the limited areas of modern log suites and core data. It is reasonable to expect, for example, that residual oil saturation after primary depletion in barrier-core facies will be different from that in inlet-fill facies of the 41-A reservoir.

Greta Reservoir— An Aggradational Barrier Sandstone

The Greta sandstone is an informal lithostratigraphic unit of the Frio Formation that is recognized by petroleum geologists as occurring across much of the middle Coastal Plain of Texas. Its distribution coincides with that of the Greta/Carancahua barrier/strandplain system of the upper Frio. The Greta sand, a massive sand body typically more than 100 ft (30 m) thick, is readily recognized by its blocky log response on SP or gamma-ray curves. Slight variations in total SP deflection and sparse, thin shale breaks suggest that the Greta consists of numerous genetic units that are a few tens of feet thick. The Greta is further characterized by its position at the top of the Frio Formation within a dominantly retrogradational facies tract capped by transgressive sediments and blanketed by the Anahuac marine shelf shale (fig. 8). Regional maps of the upper Frio sands, including the Greta, show strongly strike-parallel trends with secondary

crosscutting contours (Galloway and others, 1982, pls. 4 and 7). As shown in figure 8, the massive Greta sand body is abruptly replaced updip by an equally thick mudstone.

The Greta sandstone is the single most productive lithostratigraphic unit of the Frio barrier/strandplain oil play (Galloway and others, 1983). Because of the great thickness of the sand body, the hydrocarbon-saturated zone, which is about 50 ft (15 m) thick in West Ranch field, encompasses only the upper part of the unit. Both base- and edge-water drives are thus possible sources of reservoir energy. Absence of well-defined, continuous bedding hinders drainage control during production.

Reservoir Characteristics and Origin

One core and several modern log suites provided the basis for description of the compositional and internal attributes of the Greta reservoir.

Sands are well to moderately sorted and uniformly fine grained. Both SP and gamma-ray curves reflect the uniform texture of the massive sand body (fig. 20). Sands are mostly structureless, locally faintly laminated and cross-laminated, and show distinct bioturbation. Pervasive, indistinct root and burrow churning are likely causes of the massive, structureless appearance of the sand. Shelly zones also occur, and carbonaceous debris is common.

Although the SP logs from nearly all production wells show some variability, differences proved too subtle for reliable recognition of multiple log patterns. Resistivity curves, however, show great variability (fig. 21). Typically one or more 20- to 40-ft (6- to 12-m) zones of high resistivity (and inferred minimal residual water saturation) occur within the saturated zone. As in the 41-A sand, whether oil or gas is the hydrocarbon phase saturating the reservoir has no apparent effect on resistivity response. Cross sections drawn parallel to the regional Greta sand-body trend show that the high-resistivity zones are laterally discontinuous lenses (pl. 2, panel 3). The Greta may be described as a massive sand matrix containing pods (or, in three dimensions, channels) of above-average hydrocarbon saturation. Average water saturation in the Greta oil zone is a rather high 45 percent (average for the Frio barrier/strandplain play is 33 percent). Assuming an average porosity of 32 percent (table 1), the background resistivity of 2 ohm-m

yields a calculated S_w of 40 percent. In contrast, the high-resistivity pods have calculated water saturations of less than 30 percent (pl. 2).

A map made by plotting the maximum measured resistivity within the Greta reservoir (fig. 22) shows that the high-resistivity zones are elongate, dip-oriented, and channellike in areal geometry. The resistivity trends mirror the secondary details in the isopach map of the reservoir, which suggests that the zones of enhanced hydrocarbon saturation are facies

related. Internal facies architecture, which is reflected by hydrocarbon saturation, and external stratigraphic attributes of the Greta sandstone typify an aggradational barrier sand body that consists mainly of amalgamated inlet fills. Extensive reworking of stable, slowly aggrading barrier islands by migrating inlets is typical. Development of a large, open lagoon as the back-barrier coastal plain foundered would also increase the volume of tidal exchange and consequently would enlarge the inlets.

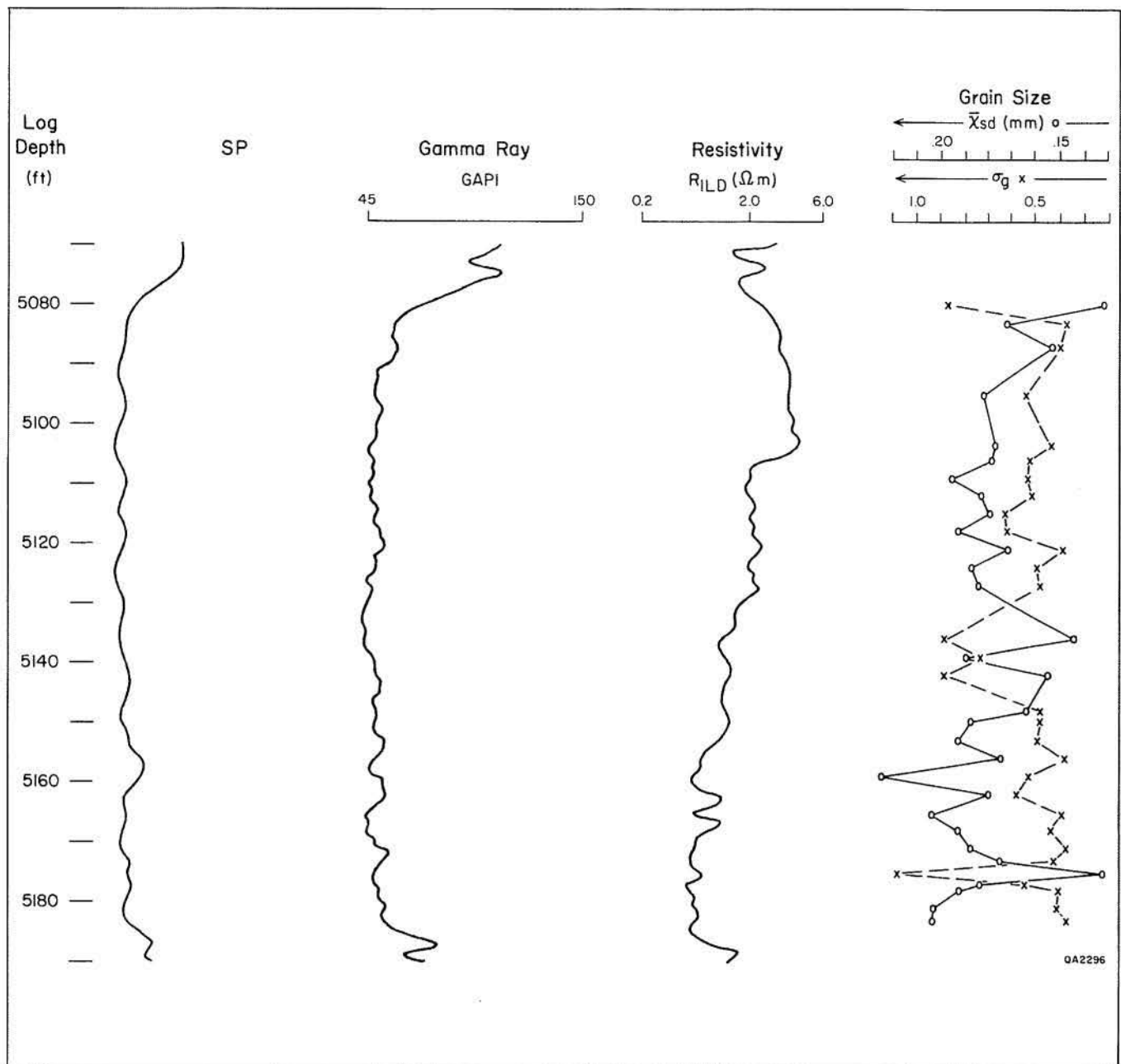


Figure 20. Typical log response and textural properties of the Greta reservoir, well A-493.

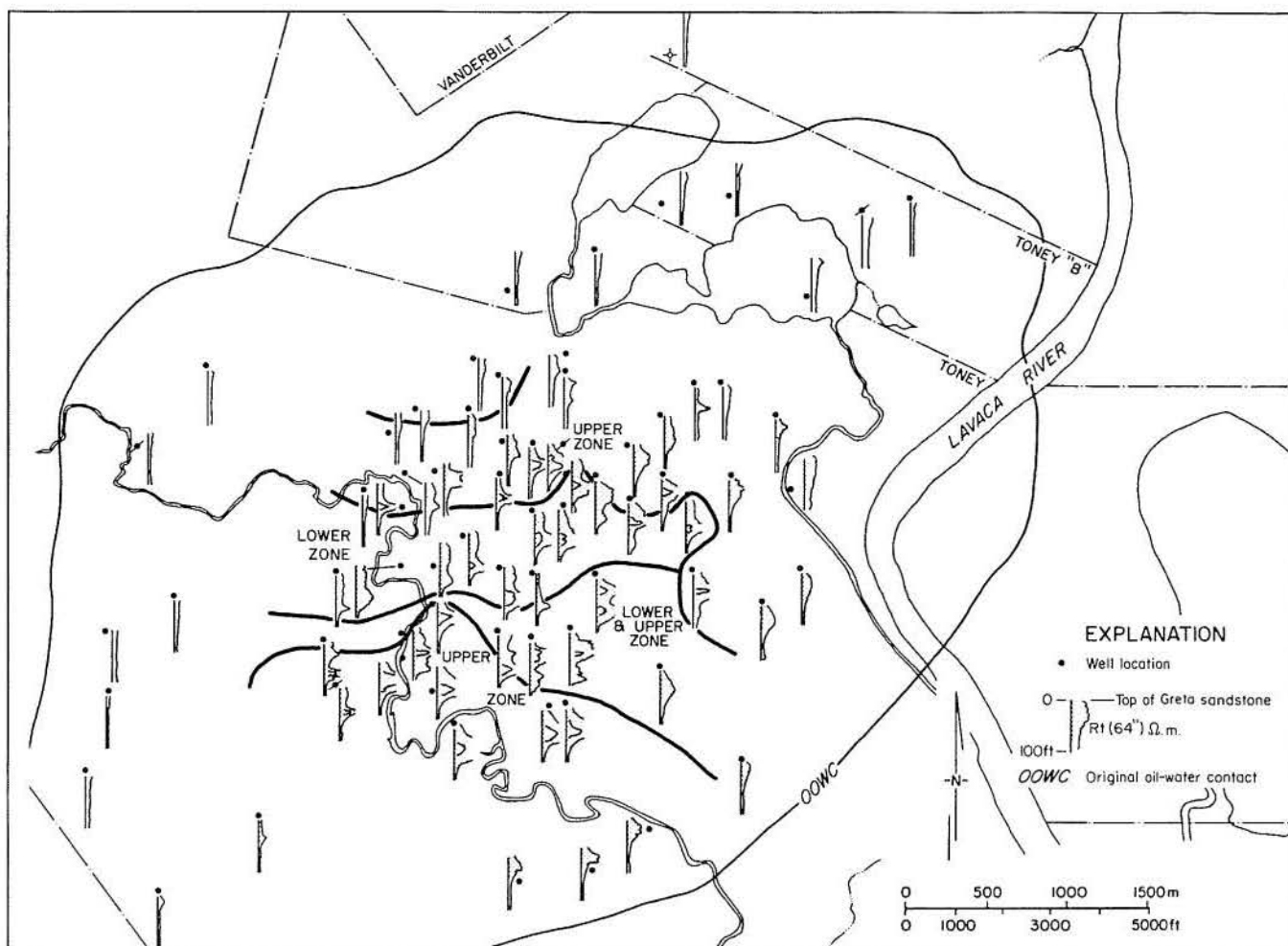


Figure 21. Map of deep-resistivity log patterns in hydrocarbon saturated portions of the Greta reservoir.

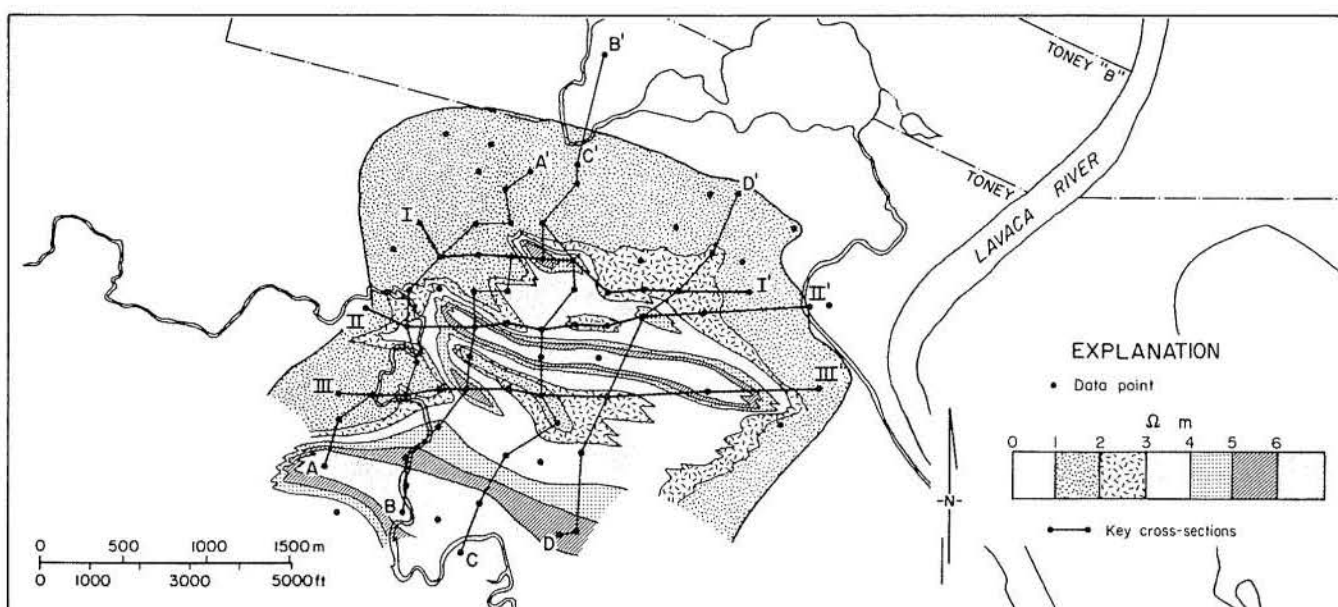


Figure 22. Distribution of maximum measured deep resistivity within hydrocarbon-saturated portions of the Greta reservoir. Dip-oriented trends are prominent.

Production History

The apparently massive, homogeneous appearance of the Greta sand is belied not only by the indirect evidence of a complex internal facies architecture but also by its production history. Highly irregular water encroachment and fingering have occurred while the reservoir has been drained. A map of water-cut patterns (fig. 23), based on numerous well tests, shows that encroachment primarily occurs as dip-elongate

fingers. Isolated "islands" having a higher oil-water ratio remain behind the irregular fingers. The pattern of fingering suggests facies influences on reservoir drainage. As with the 41-A example, however, site-specific interpretation of water-cut and gas-oil ratio patterns also requires knowledge of perforation intervals.

To maximize recovery efficiency, which is projected to be 42 percent, the operator subdivided the Greta reservoir into arbitrary 10-ft slices. A detailed three-dimensional record of perforation



Figure 23. Map of water-cut for wells producing in the Greta reservoir, June 1977. Prominent fingers of water incursion are shown by the arrows.

and depletion history is maintained by mapping each slice individually. Such mapping has shown that, despite the apparent lack of bedding and consequent potential for base-water encroachment, horizontal intrastratal fingering characterizes depletion of the Greta reservoir. Thus, both original hydrocarbon saturation and drainage patterns are directly related to the inlet-dominated depositional architecture of the Greta aggradational barrier complex.

Glasscock Reservoir— A Transgressive Barrier Sandstone

The regional cross section shows the Glasscock sandstone to be a thin unit lying along the landward fringe of the transgressive shale capping progradational cycle "C" (fig. 8). Its stratigraphic position is appropriate to that resulting from the transgression and stabilization of a barrier island.

The Glasscock sandstone is characterized by a subdued SP log response. To map sand-body geometry, the SP cutoff used to define net sandstone was shifted from the conventional 50 percent maximum deflection to 25 percent of the maximum clean-sandstone deflection from the shale baseline. Despite its thinness, the zone is widespread in the field area; the Glasscock is the

most extensive oil producing horizon in West Ranch field. The reservoir can be further subdivided into three persistent subzones (fig. 24) that can be correlated throughout most of the field. Most of the sand (as defined by the SP log) lies within subzone 1 at the top of the sandstone unit. In plan view, the Glasscock sandstone displays landward-bifurcating sand thicks and an overall thinning from its downdip margin within the field (fig. 25). However, wells at the oil-water contact along the southeast margin of the field also penetrated a much thinner Glasscock sand body. Coincidentally with the changes in thickness and map pattern, SP log motifs (fig. 25) shift from type A (transitional top), to mixed types B and C (transitional base and sharp top, "stairstep" subzones), to type D (serrate or irregular).

Reservoir Characteristics and Origin

Internally the Glasscock sandstone appears massive and homogeneous. Faint parallel lamination and burrows are apparent in the core (fig. 24). Scattered oystershell also occurs. Most prominent in the sandstone is the abundant pedogenic or diagenetic clay matrix, which has played a major role in reducing the porosity and permeability of the reservoir (table 1). Effects of the clay are also indicated by the dissimilarity of the SP and gamma-ray log profiles (fig. 24). The

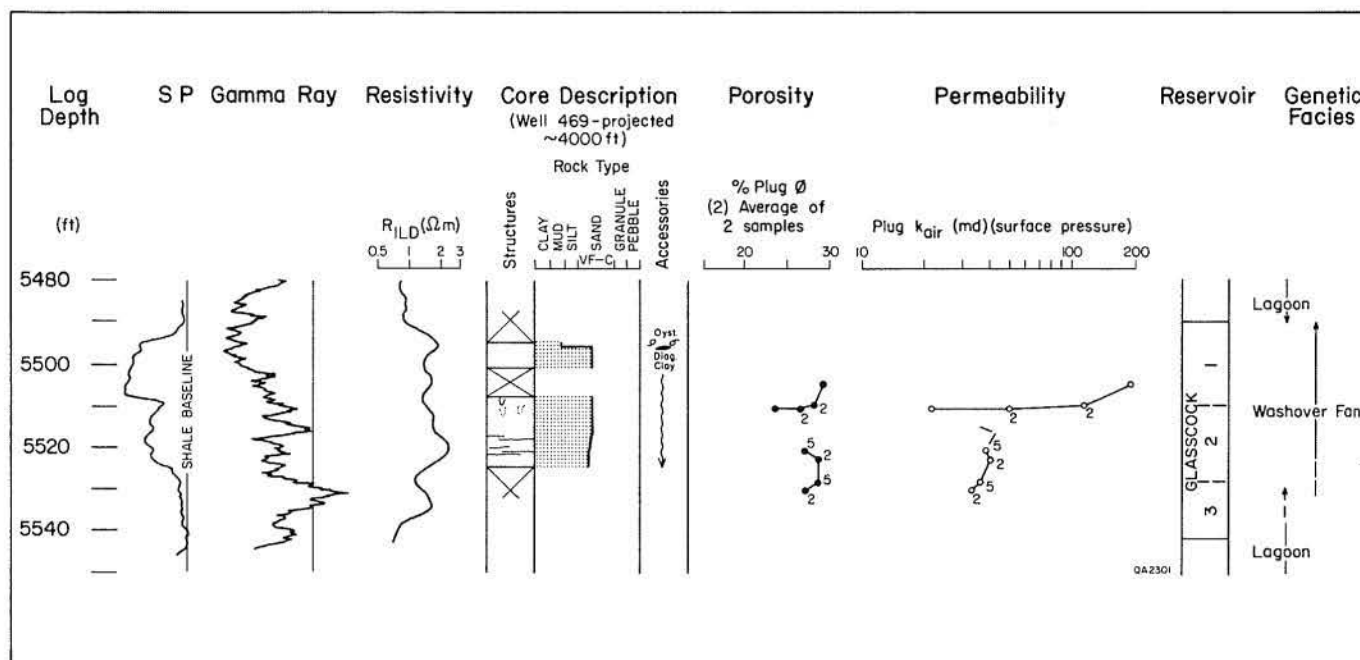


Figure 24. Log response, internal features, and petrophysical properties typical of the Glasscock reservoir, well A-476. The sand body can be subdivided into three thin zones throughout the field area.



Figure 25. Net-sand isolith map of the Glasscock reservoir. Contours emphasize data derived from newer and better quality SP logs.

relatively limited volume and the lower permeability of the Glasscock explain the lack of a strong natural water drive, which is typical of most Frio barrier-island reservoirs. Limited data from core plugs suggest that the three subzones have different reservoir properties (fig. 24).

Stratigraphic setting, sand-body geometry, and internal features support the interpretation of

the Glasscock reservoir as a complex of large washover fans (fig. 26) similar to those of modern coastal barriers described by Andrews (1970), Wilkinson (1975), and Wilkinson and Basse (1978). Component facies in modern washover fans include the shallow washover channel and poorly developed inlet fill typical of transgressive barriers, back-barrier vegetated flat, eolian flat,

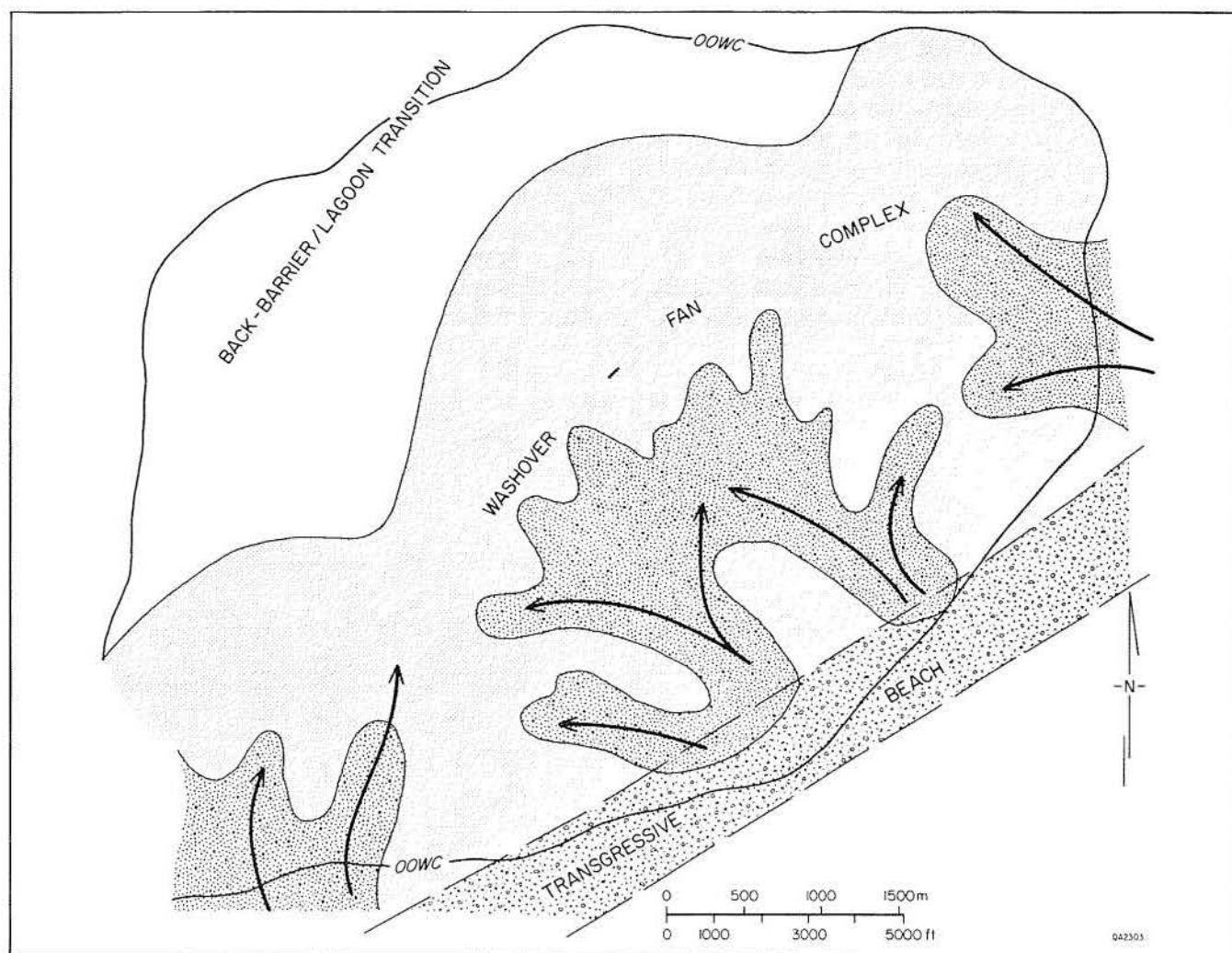


Figure 26. Interpreted depositional elements of the Glasscock sand in the main field area.

and marginal grassflat. The sandstone grades landward into and is enclosed within lagoonal mudstones. It grades basinward into erosional beach and overlying, inverted shoreface deposits. Transitional facies, such as the shallow-water grassflats, consist of muddy sand and may be a major component of subzones 1 and 2.

Hydrocarbon Distribution and Production History

The Glasscock sandstone contrasts with other West Ranch reservoirs because it is a relatively low permeability (300 to 400 md), argillaceous reservoir exhibiting a poor water drive. Highest permeability appears to occur at or near the top of the sand body in subzone 1. Reservoir characteristics are further indicated by the patterns of hydrocarbon saturation interpreted from resis-

tivity logs. Highest oil saturations are found in subzone 1 (pl. 2, panel 4); intermediate saturations in subzone 2, and lowest saturations in subzone 3, at the base of the reservoir. Local lenses (channels in plan view) of high resistivity (lower S_w) cut through subzone 1 and correspond to washover-fan channel fills. They are commonly coincident with SP log motif A, indicating a gradational, or upward-fining, sand to shale boundary. A few thin, highly resistant zones, such as in well A-397 (NE-SW cross section, pl. 2, panel 4), are probably tight, carbonate-cemented zones produced by solution and reprecipitation of shell lags within the washover channels. The generally low measured resistivity values typical of most of the reservoir are consistent with the high (41 percent) average water saturation.

Although it has well-developed horizontal stratification and greater lateral uniformity than

either the 41-A or the Greta reservoir, the Glasscock sandstone exhibits a comparably irregular hydrocarbon saturation and drainage history. Poorer reservoir quality and less effective natural reservoir energy led to initiation of a water-injection program by the operator. Water is injected into the reservoir along the periphery of the gas cap to maintain reservoir pressure and to prevent expansion of the gas cap into the oil-bearing zone. The advance of the injection front into the oil zone has been quite irregular (fig. 27).

Inferred flow lines from injection wells closely parallel facies trends, particularly within subzone 1. Injected water preferentially flows into and along more permeable conduits, particularly the washover channels. Such funneling of flow into sand trends is especially prominent along the southwest margin of the field (compare trends on figures 25 and 27). The Glasscock sandstone has the lowest projected recovery efficiency, only 39 percent of the oil in place, of all the major West Ranch field reservoirs.

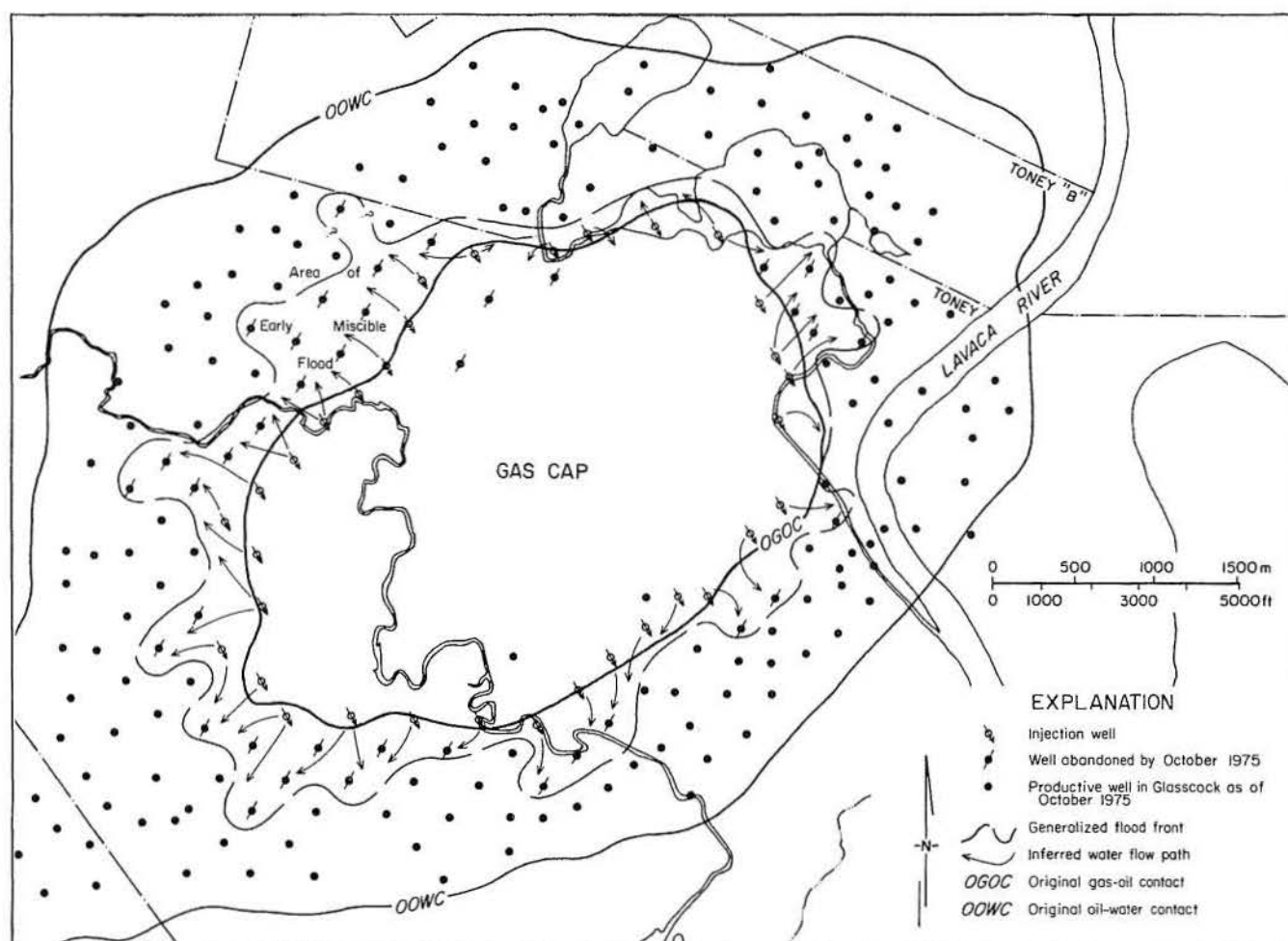


Figure 27. Geometry of water-flood front following 9 years of water injection along the gas-oil contact. Inferred flow paths are shown by the arrows.

DISCUSSION AND CONCLUSIONS

Reservoir sand bodies of microtidal barrier-island origin are a complex mosaic of individual depositional elements. Fore-barrier, barrier-core, and back-barrier facies assemblages can be distinguished. The examples discussed here show

that in the Frio, as in the Jackson barrier/strandplain systems of the Texas Gulf Coast, Tertiary barrier-island deposits closely resemble their Holocene counterparts in thickness, areal extent, and internal characteristics.

All three barrier-island reservoirs display the same basic depositional elements:

1. A uniform, strike-trending facies complex consisting of barrier-core, washover/barrier-flat, and flood-tidal-delta sands, and
2. An erosionally based, lenticular, non-uniform, dip-trending, channel-fill complex, consisting of tidal-inlet, washover-channel, or tidal-channel facies elements, that transects the barrier trend.

The dimensions (thickness and areal geometry) of Frio barrier-island reservoirs are comparable to those of their modern analogs. Thus, facies studies of the Holocene barriers allow reconstruction of likely internal reservoir facies patterns and prediction of petrophysical trends. Three reservoir facies models that compare and contrast inlet fill, tidal-channel fill, and washover-channel fill and their bounding barrier facies are shown in figures 28A, 29A, and 30A. It is important to note that at common well spacings of 20 or 40 acres, facies boundaries partially isolate many well penetrations of such barrier reservoirs.

Distribution of reservoir properties—especially permeability and pore geometry—that determine hydrocarbon saturation, relative fluid mobility, and drainage patterns are established by the original complex depositional mosaic. Consequently, each facies model defines a comparable reservoir engineering model of the reservoir (figs. 28A through 30A). Distribution, relative position, abundance, trend, anisotropy, bedding attributes, and nature of boundaries of permeability units and impermeable beds and lenses are directly related to the depositional patterns. During burial, the original reservoir qualities are modified by compaction of fine-grained intervals, precipitation of intergranular cements, and leaching of framework grains. However, in loosely consolidated sandstones, such as the shallow Frio, surviving gradients in reservoir quality mimic the original, texturally defined gradients. Although permeability contrasts can be great (orders of magnitude), few truly impermeable beds occur. Deeply buried Frio barrier sandstones, or older stratigraphic units, may have undergone advanced burial diagenesis, resulting in overall porosity and permeability reduction and concomitant accentuation of facies-defined permeability contrasts, anisotropies, and isolation by sealing beds.

In highest quality barrier-island reservoirs, such as the 41-A and Greta, recovery efficiency is generally high, commonly approaching 50 per-

cent of the oil in place (Galloway and others, 1983). However, as demonstrated by the Glasscock sandstone, comparatively poor reservoir quality and less effective natural reservoir energy reduce recovery. Despite the appearance of good pressure continuity, migration of injected fluids is determined by internal facies architecture of the reservoir.

Many authors have argued that improved recovery of hydrocarbons from typically complex sandstone reservoirs necessitates a thorough integration of sedimentologic data (Harris, 1975; Harris and Hewitt, 1977; Weber and others, 1978). Indeed internal heterogeneities of the reservoir are a direct and interpretable product of the original association of depositional environments and resultant component facies. This study has:

1. Demonstrated the complex internal facies patterns and their effects on the initial distribution and mobility of hydrocarbons within barrier-island reservoirs.
2. Illustrated working methods for recognizing and delineating intrareservoir facies elements using detailed isolith mapping and various types of log-pattern mapping.
3. Showed that resistivity and other indirect measurements may provide semiquantitative descriptions of reservoir parameters, such as permeability, that are necessary for accurate reservoir simulation and design of enhanced recovery programs. Use of derived or empirical relationships among sediment texture, irreducible water saturation, porosity, permeability, and internal bedding geometry, when calibrated with limited core control, greatly increases the potential detail of reservoir description. Weber and others (1978) provide an excellent illustration of the use of such approaches in the design of a waterflood program for a barrier-bar reservoir in the Tertiary deposits of the Niger delta.
4. Provided summary models of types of intrareservoir facies and petrophysical variability that are applicable to microtidal barrier-island reservoirs. The pictorial models (figs. 28 through 30) illustrate common facies associations and resultant heterogeneities within barrier-island sand bodies. They are visual guides for recognition of similar facies mosaics in comparable reservoirs of the Frio Formation and in analogous barrier-island depositional systems of the Gulf Coast and other basins.

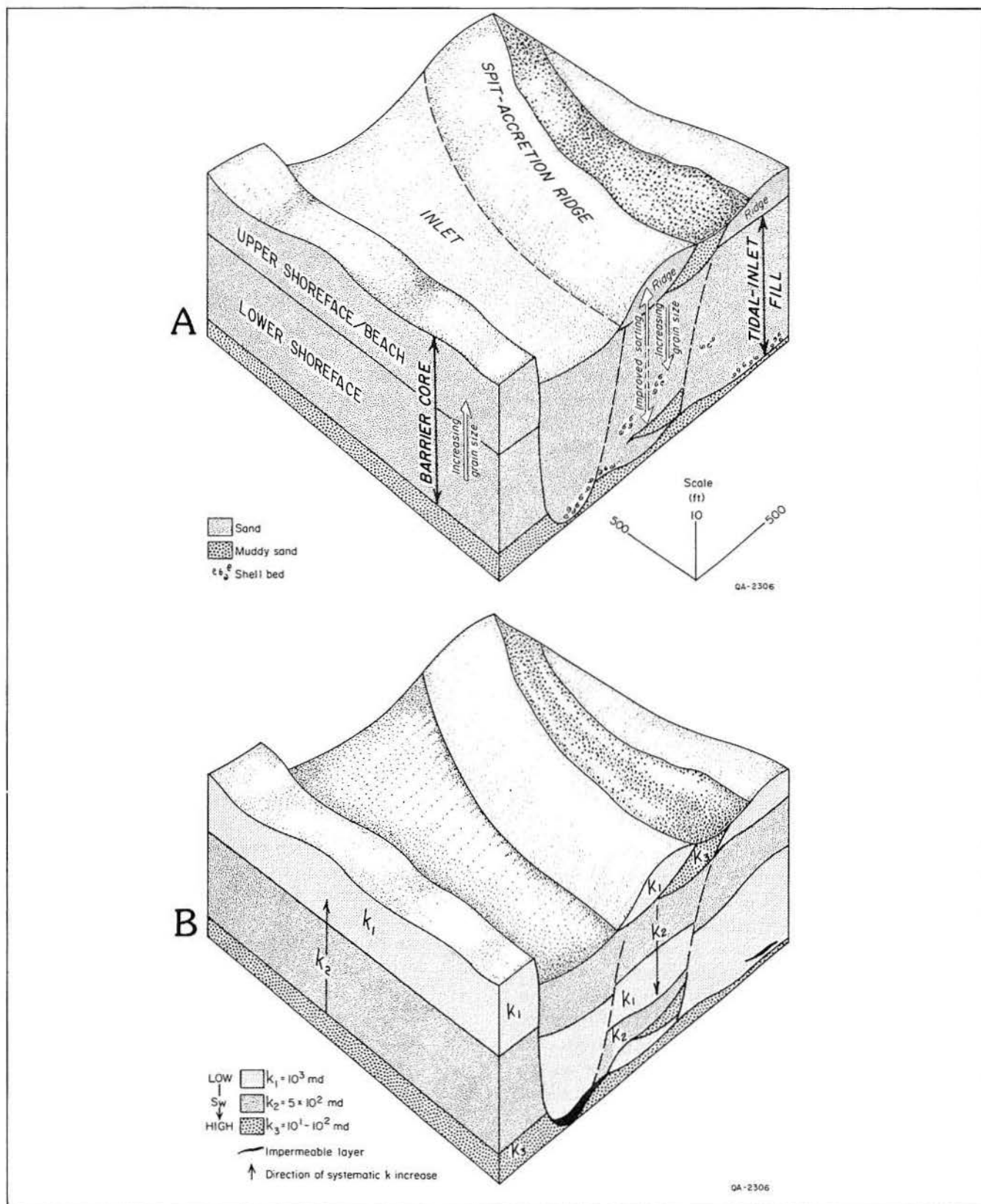


Figure 28. Reservoir model of the barrier-core and inlet-fill facies complex. A. Depositional environments and textural trends. B. Reservoir compartments and permeability trends. Permeability values shown are typical of those in the Frio barrier/strandplain system. Absolute values would differ in different stratigraphic units, but trends and relative values would remain similar.

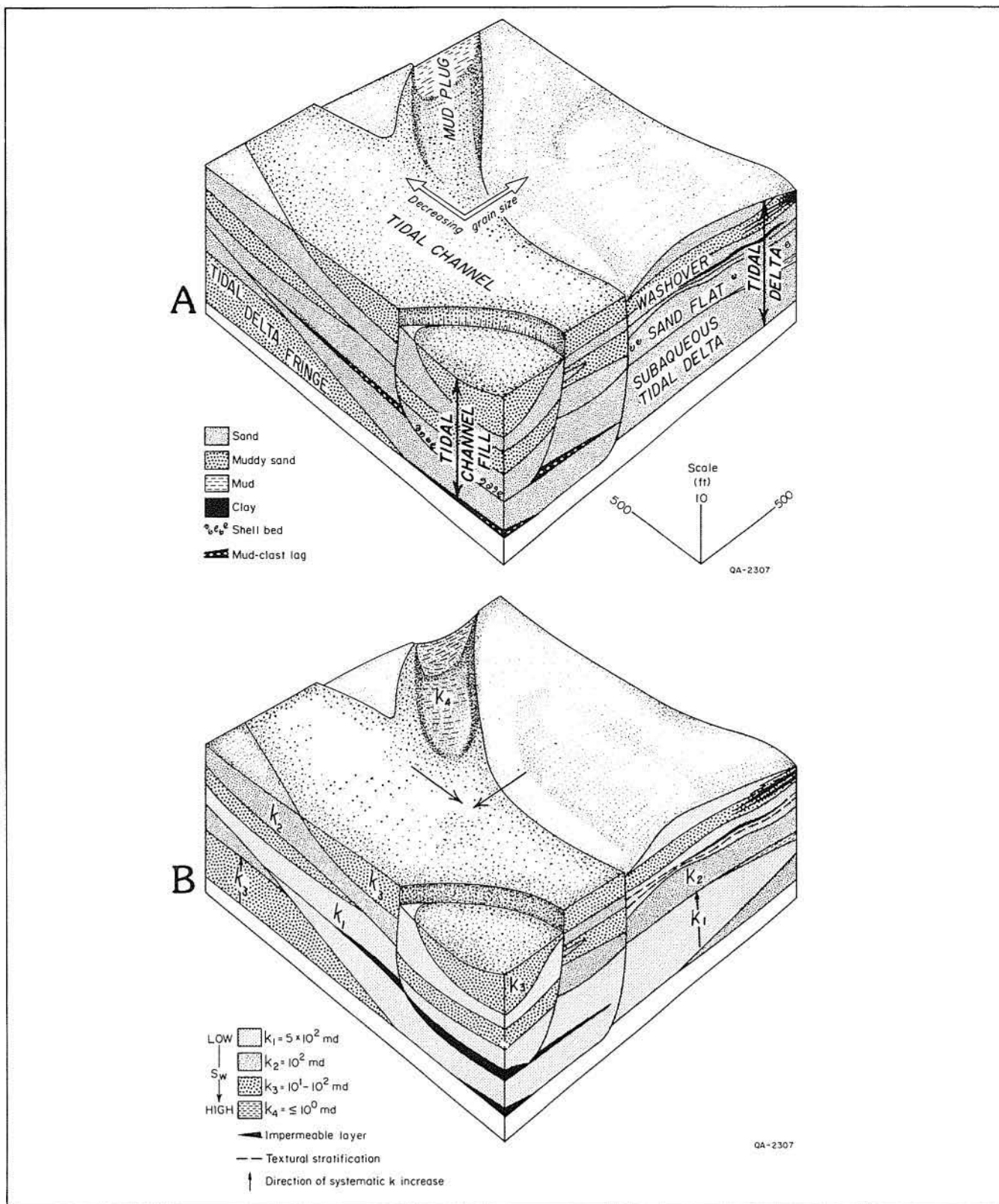


Figure 29. Reservoir model of tidal-channel fill and associated tidal-delta and back-barrier facies mosaic. A. Depositional environments, bedding geometry, and textural trends. B. Reservoir compartments, stratification, and permeability trends. Permeability values shown are typical of those in the Frio barrier/strandplain system. Absolute values would differ in different stratigraphic units, but trends and relative values would remain similar.

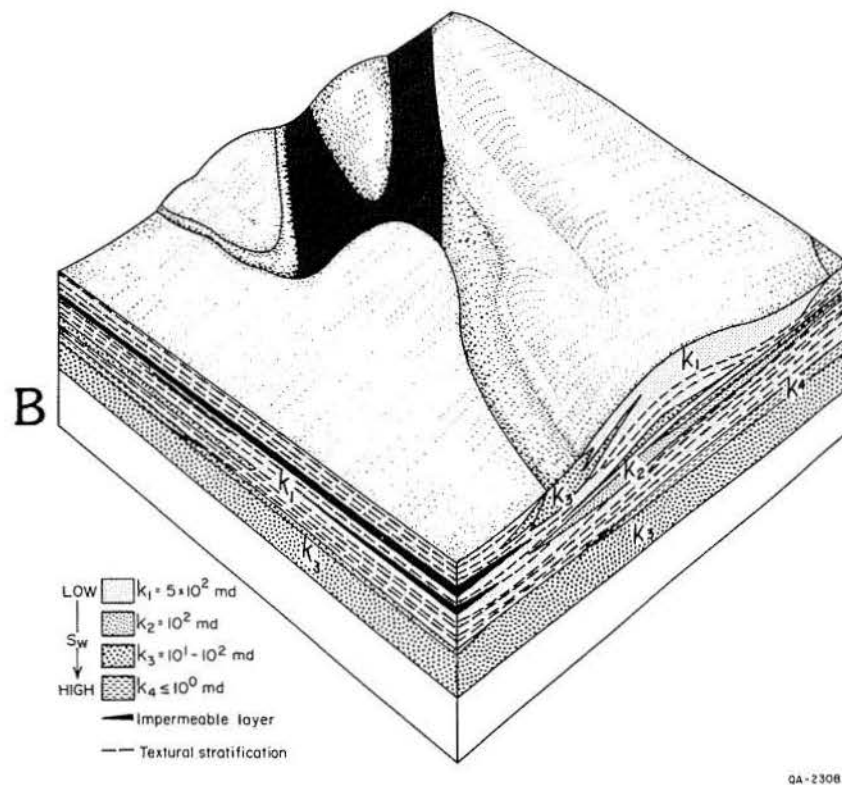
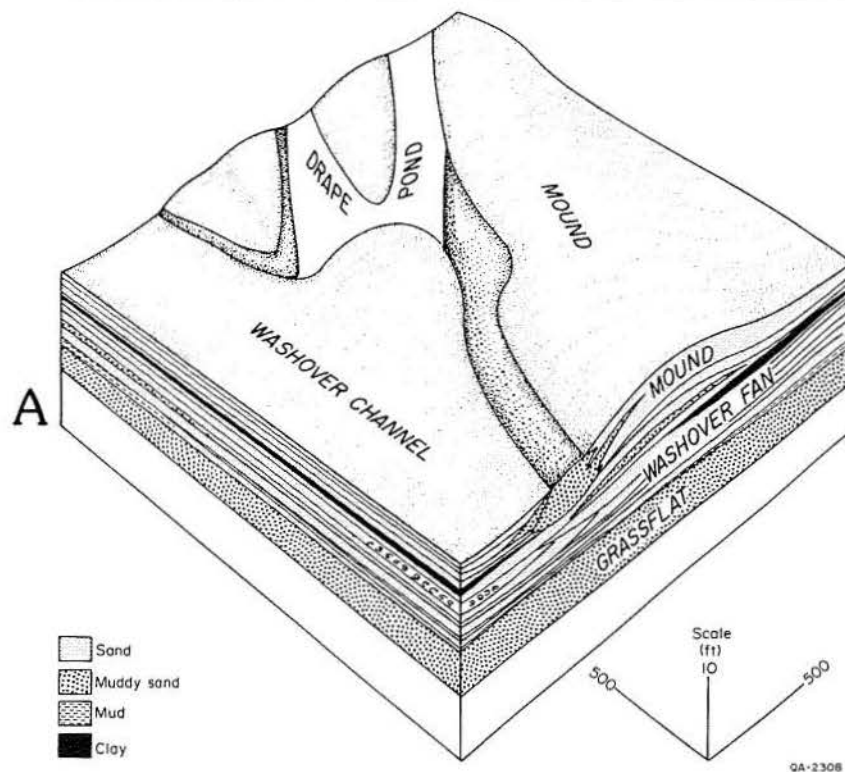


Figure 30. Reservoir model of washover-fan and associated back-barrier facies. A. Depositional environments, bedding geometry, and textural trends. B. Reservoir compartments, stratification, and permeability trends. Permeability values shown are typical of those in the Frio barrier/strandplain system. Absolute values would differ in different stratigraphic units, but trends and relative values would remain similar.

ACKNOWLEDGMENTS

We express special appreciation to Mobil Oil Corporation for providing much data on the West Ranch field; the cooperation of Mobil personnel was instrumental to this research. Richmond Vaught, Robert Timmons, Carl Dimon, and James Dixon, in particular, contributed their time and effort to data acquisition and provided thoughtful discussions and review of the interpretations presented here.

The manuscript was reviewed by L. F. Brown, Jr., Jules R. DuBar, R. A. Morton, R. J. Finley, M. P. R. Light, and Mary L. W. Jackson of the Bureau of Economic Geology. Figures were drafted by Jana Brod, Jamie McClelland, and Richard M. Platt, under the supervision of R. L. Dillon. Text illustration photography was by James A. Morgan. The manuscript was edited by Amanda R. Masterson. Word processing and typesetting were by Shelley G. Gilmore and Phyllis J. Hopkins, under the supervision of Lucille C. Harrell. Margaret L. Evans designed the publication.

REFERENCES

- Andrews, P. B., 1970, Facies and genesis of a hurricane-washover fan, St. Joseph Island, central Texas coast: The University of Texas at Austin, Bureau of Economic Geology Report of Investigations No. 67, 147 p.
- Bauernschmidt, A. J., Jr., 1944, West Ranch oil field, Jackson County, Texas: American Association of Petroleum Geologists Bulletin, v. 28, no. 2, p. 197-216.
- Bernard, H. A., Major, C. G., Jr., Parrott, B. S., and LeBlanc, R. J., 1970, Recent sediments of southeast Texas, a field guide to the Brazos alluvial and deltaic plains and the Galveston barrier island complex: The University of Texas at Austin, Bureau of Economic Geology Guidebook 11, 132 p.
- Galloway, W. E., Ewing, T. E., Garrett, C. M., Tyler, Noel, and Bebout, D. G., 1983, Atlas of major Texas oil reservoirs: The University of Texas at Austin, Bureau of Economic Geology Special Publication, 139 p.
- Galloway, W. E., and Hobday, D. K., 1983, Terrigenous clastic depositional systems: applications to petroleum, coal, and uranium exploration: New York, Springer-Verlag, 423 p.
- Galloway, W. E., Hobday, D. K., and Magara, Kinji, 1982, Frio Formation of the Texas Gulf Coast Basin—depositional systems, structural framework, and hydrocarbon origin, migration, distribution, and exploration potential: The University of Texas at Austin, Bureau of Economic Geology Report of Investigations No. 122, 78 p.
- Harris, D. G., 1975, The role of geology in reservoir simulation studies: Journal of Petroleum Technology, v. 27, p. 625-632.
- Harris, D. G., and Hewitt, C. H., 1977, Synergism in reservoir management—the geologic perspective: Journal of Petroleum Technology, v. 29, p. 761-770.
- Hayes, M. O., and Kana, T. W., 1976, Terrigenous clastic depositional environments: University of South Carolina, Department of Geology, Coastal Research Division, Technical Report No. 11-CRD, 302 p.
- Heron, S. D., Jr., Moslow, T. F., Berelson, W. M., Herbert, J. R., Steele, G. A., III, and Susman, K. R., 1984, Holocene sedimentation of a wave-dominated barrier-island shoreline: Cape Lookout, North Carolina: Marine Geology, v. 60, p. 413-434.
- Hubbard, D. K., Oertel, G. F., and Nummedal, Dag, 1979, The role of waves and tidal currents in the development of tidal-inlet sedimentary structures and sand body geometry: examples from North Carolina, South Carolina, and Georgia: Journal of Sedimentary Petrology, v. 49, no. 4, p. 1073-1092.
- Kraft, J. C., and John, C. J., 1979, Lateral and vertical facies relations of transgressive barrier: American Association of Petroleum Geologists Bulletin, v. 63, no. 12, p. 2145-2163.
- Kumar, Naresh, and Sanders, J. E., 1974, Inlet sequence: a vertical sequence of sedimentary structures and textures created by the lateral migration of tidal inlets: Sedimentology, v. 21, p. 491-532.
- Morton, R. A., and McGowen, J. H., 1980, Modern depositional environments of the Texas coast: The University of Texas at Austin, Bureau of Economic Geology Guidebook 20, 167 p.
- Penland, Shea, and Suter, J. R., 1983, Transgressive coastal facies preserved in barrier island retreat paths in the Mississippi River delta plain: Gulf Coast Association of Geological Societies Transactions, v. 33, p. 367-381.
- Pittman, E. D., 1979, Porosity, diagenesis, and productive capability of sandstone reservoirs, in Scholle, P. A., and Schluger, P. R., eds., Aspects of diagenesis: Society of Economic Paleontologists and Mineralogists Special Publication No. 26, p. 159-173.
- Schlumberger Offshore Services, 1974, A guide to well site interpretation for the Gulf Coast: Schlumberger, 55 p.
- Schmidt, Volkmar, McDonald, D. A., and Platt, R. L., 1977, Pore geometry and reservoir aspects of secondary porosity in sandstones: Bulletin of Canadian Petroleum Geology, v. 25, p. 271-290.
- Tyler, Noel, and Ambrose, W. A., in press, Facies architecture and production characteristics of strandplain reservoirs in the Frio Formation, Texas: The University of Texas at Austin, Bureau of Economic Geology Report of Investigations.

Weber, K. J., Klootwijk, P. H., Konieczek, J., and van der Vlugt, W. R., 1978, Simulation of water injection in a barrier-bar-type, oil rim reservoir in Nigeria: *Journal of Petroleum Technology*, v. 30, p. 1555-1565.

Wilkinson, B. H., 1975, Matagorda Island, Texas: the evolution of a Gulf Coast barrier complex: *Geological Society of America Bulletin*, v. 86, no. 7, p. 959-967.

Wilkinson, B. H., and Basse, R. A., 1978, Late Holocene history of the central Texas coast from Galveston Island to Pass Cavallo: *Geological Society of America Bulletin*, v. 89, no. 10, p. 1592-1600.

APPENDIX

Production History of Barrier-Island Reservoirs, West Ranch Field (based on information in hearing files of the Oil and Gas Division of the Railroad Commission of Texas)

Greta Sandstone

Total sand thickness of the Greta reservoir commonly exceeds 100 ft (30 m). The oil column is 46 ft (15 m) thick. The oil zone is totally underlain by water. However, water encroachment shows that edge-water drive is the main energy source of the reservoir. The original reservoir pressure was 2,357 psig. Pressure declined only 195 psi from 1938 to 1967.

Because of the thickness of the sand, the operator divided the pay zone into eight 10-ft layers. Drainage is controlled by well production and plug-back and monitored by well tests. The layer control method provides efficient reservoir management and minimizes the chances of bypassing oil.

Glasscock Sandstone

The Glasscock is a gas-cap, oil-rim reservoir. The original gas cap was about one-third the size of the oil zone. Reservoir energy has been estimated by the operator to be about 95 percent gas-cap drive and 5 percent water drive. Original reservoir pressure was 2,575 psia. Isobaric mapping during the primary production stage supports the gas-cap expansion mechanism.

Pressure distribution generally followed the reservoir structure and showed no major anomaly throughout the field. Pressure declined to 2,000 psig in 1966. The operator started to inject water at the original gas-oil contact, thereby displacing oil in a downdip direction. Water was injected into the structurally high part of the reservoir because high water saturation in the low-structure area would result in inefficient formation of an oil bank and poor injection response. Low water saturation high on the structure meant that

higher relative oil permeability and an oil bank formed through water injection were expected. A pilot water-injection project indicated the economic feasibility of the method.

41-A Sandstone

The 41-A reservoir has a strong natural water drive. The original reservoir pressure was 2,625 psig, and during the first 20 years of production, pressure decline was gradual. Beginning in 1961, higher reservoir withdrawal caused a sharp pressure decline and reservoir pressure fell to 2,100 psig by December 1972. Dramatic increases in water production and gas-oil ratio showed that the natural water drive was insufficient to maintain the pressure at the increased withdrawal rate (45,000 bbl/day by December 1972).

Water injection was initiated in May 1973 for pressure maintenance. Salt water from various zones in the West Ranch field is injected in a downdip, peripheral pattern, under maximum pressure of 1,700 psia, at an estimated maximum rate of 5,000 bbl/day.

After water injection commenced reservoir pressure increased and has been maintained at more than 2,100 psig with uniform pressure distribution. Isobaric maps show no evidence of anomalous gradients across the field. Average producing gas-oil ratio was lowered from 751 cu ft/bbl in 1972 to 538 cu ft/bbl in 1977.

In November 1977, the operator proposed an infill development program to recover additional reserves by drilling several wells on 10-acre spacing. Success of this effort has not been discussed by the operator.